



Vegetation change across the Drake Passage region linked to late Eocene cooling and glacial disturbance after the Eocene-Oligocene Transition

5 Nick Thompson¹, Ulrich Salzmann¹, Adrián López-Quirós^{2,3}, Peter K. Bijl⁴, Frida S. Hoem⁴, Johan Etourneau³, Marie-Alexandrine Sicre⁵, Sabine Roignant⁶, Emma Hocking¹, Michael Amoo¹, Carlota Escutia³

¹Department of Geography and Environmental Sciences, Northumbria University, Newcastle upon Tyne, UK.

²Department of Geoscience, Aarhus University, Høegh-Guldbergs Gade 2, 8000, Aarhus C, Denmark.

10 ³Instituto Andaluz de Ciencias de la Tierra, CSIC-Universidad de Granada, Granada, Spain.

⁴Department of Earth Sciences, Utrecht University, Utrecht, The Netherlands.

⁵Sorbonne Universites (UPMC, Univ. Paris 06)-CNRS-IRD-MNHN, LOCEAN Laboratory, Paris, France.

⁶Institut Universitaire Européen de la Mer, Plouzane, France.

Correspondence to: Nick Thompson (alasdair.thompson@northumbria.ac.uk)

15 **Abstract.** The role and climatic impact of the opening of the Drake Passage and how it affected both marine and terrestrial environments across the Eocene-Oligocene Transition (EOT ~34 Ma) period remains poorly understood. Here we present new terrestrial palynomorph data compared with recently compiled lipid biomarker (*n*-alkane) data from Ocean Drilling Program (ODP) Leg 113 Site 696 drilled on the margin of the South Orkney Microcontinent in the Weddell Sea, to investigate changes in terrestrial environments and paleoclimate across the late Eocene and early Oligocene (~37.6-32.2 Ma). Early late Eocene
20 floras and sporomorph-based climate estimates reveal *Nothofagus*-dominated forests growing under wet temperate conditions, with mean annual temperature (MAT) and precipitation (MAP) around 13°C and 1660 mm, respectively. A phase of latest Eocene terrestrial cooling at 35.5 Ma reveals a decrease in MAT by around 2°C possibly linked to the opening of the Powell Basin. This is followed by an increase in Mesozoic sporomorphs together with a shift in terrestrial biomarkers and sedimentological evidence indicating ice expansion to coastal and shelf areas approximately 34.1 million years ago. However,
25 major changes to the terrestrial vegetation at Site 696 did not take place until the early Oligocene, where there is a distinct expansion of gymnosperms and cryptogams accompanied by a rapid increase in taxa diversity following 33.5 Ma. This unusual expansion of gymnosperms and cryptogams is suggested to be linked to environmental disturbance caused by repeat glacial expansion and retreat, which facilitated the expansion of conifer and ferns. We conclude that the timing of glacial onset rather suggests that the event at site 696 is linked to the global cooling at the EOT and that latest Eocene regional cooling cannot
30 directly be linked. Therefore, confirming that the opening of ocean gateways alone did not trigger Antarctic glaciation, even if ocean gateways may have played a role in stepwise cooling before the EOT.



1. Introduction

The Cenozoic progression from greenhouse to icehouse climate conditions was accompanied by the establishment of the Antarctic ice sheet around the Eocene-Oligocene Transition (EOT 34.44-33.65 Ma; e.g., Hutchinson et al., 2021). This change in Earth climate state is evidenced by a prominent excursion in oxygen isotope ratios from marine biogenic calcite (e.g., Zachos et al., 2001, 2008; Westerhold et al., 2020) during the Earliest Oligocene Oxygen Isotope Step (EOIS ~33.65Ma; Hutchinson et al., 2021). The possible causes of the onset of Antarctic glaciation are poorly understood and ambiguity remains as to whether a single or combination of factors and feedbacks drove the Cenozoic climate transition (e.g., DeConto and Pollard, 2003; Coxall and Pearson, 2007). Uncertainties particularly remain over the role of the opening and deepening of the Drake Passage on the development of the Antarctic Circumpolar Current (ACC), and how this affected both marine and terrestrial environments (Scher and Martin, 2008; Houben et al., 2019). Today the ocean currents and the ACC exerts a strong influence on the Earth's climate system, playing an important role in the global distribution of heat, nutrients, salt, carbon, as well as in the gas exchange between the atmosphere and the ocean. Given that unabated anthropogenic warming is expected to cause a poleward shift of the ACC and potentially weaken thermohaline circulation (Zhang and Delworth, 2005) this study forms part of a wider need to fully understand the Earth climate system in order to better predict future stability of the Antarctic ice sheet.

A major obstacle in understanding the role of the opening Drake Passage and ocean currents in Cenozoic climate change has been the lack of well dated continuous records spanning the EOT from the region. Here we present new terrestrial palynomorph data from Ocean Drilling Program (ODP) Leg 113 Site 696 Hole B (herein referred to as Site 696), containing a well recovered EOT section, depicting changes in terrestrial environments and paleoclimate from the late Eocene to early Oligocene (~37.6-32.2 Ma; Houben et al., 2013, 2019). Vegetation composition, structure and diversity patterns are reconstructed along with sporomorph-based quantitative climate estimates in order to explore the timing and nature of vegetation and climate change across the northern Antarctic Peninsula region and South Orkney Microcontinent (SOM). The results are compared with recently compiled lipid biomarker (*n*-alkane) data (López-Quirós et al., in review), and dinoflagellate cyst data (Houben et al., 2013) to better understand shifts in marine as well as terrestrial environments and the source of terrestrial versus aquatic organic matter. Our results reveal a possible link between changing oceanographic conditions and latest Eocene terrestrial cooling around 35.5 Ma, before glacial onset in the region.

2. Materials and Methods

Site 696, hole B was drilled on the south-eastern margin of the SOM (Fig.1; latitude: 61°50.959'S, longitude: 42°55.996'W) at 650m water depth, as part of ODP Leg 113 in 1987 (Barker et al., 1988). The recovered section consists of late Eocene to Quaternary hemipelagic (214-0 mbsf), diatomaceous (530-214 mbsf), and terrigenous (645.4-530 mbsf) sediments (Barker et al., 1988; Wei and Wise, 1990; Gersonde and Burekle, 1990; López-Quirós et al., 2019, 2020, in review) and is divided into



65 seven lithological units (I-VII), primarily based on composition and diagenetic maturity of sediments (Fig. 2; Barker et al., 1988). This study focuses on pollen and spores recovered from the terrigenous unit VII (cores 113-696B-62R through 113-696B-53R; Fig. 2). Age-control based primarily on the presence of calcareous nannofossils (Wei and Wise, 1990 *sensu* Villa et al., 2008; and a revised dinoflagellate cysts age model (Houben et al., 2013, 2019), places the studied section at 33.2 to 37.6 Ma (Table 1), with sediments encompassing the EOT and EOIS event well recovered between 571.5 mbsf to 569.1 mbsf (Houben et al., 2013).

70

A total of 35 samples from the late-middle Eocene to earliest Oligocene (643.73-520.88 mbsf) were analysed for their pollen and spore content. Raw data collected is available from the PANGEA database (Thompson et al., awaiting validation). All palynological slides were prepared using standard chemical palynological processing techniques following the protocols at the University of Northumbria, Department of Geography and Environmental Sciences and the Laboratory of Palaeobotany and the Laboratory of Palaeobotany and Palynology of Utrecht University. Slides were analysed using a Leica DM500 and Leica DM2000 transmitted light microscopes at 200x and 1000x magnification. Where possible, counts of 300 (excluding reworked grains) sporomorphs were made. Only samples containing 50 or more in situ sporomorphs were used for further analysis and evaluation.

80 Identification and taxonomic classification of sporomorphs were carried out primarily following Cookson (1950), Cookson and Pike (1954), Dettmann et al. (1990), Dettmann and Jarzen (1996), Truswell and Macphail (2009) and Raine et al. (2011). Botanic and taxonomic affinities used to identify the Nearest Living Relatives (NLR) of fossil species were established mainly after Truswell and Macphail (2009) and Raine et al. (2011) and references therein (Table 2.). Identification of reworked grains are mainly based on the age-restriction of the species, with species older than Eocene or Oligocene (e.g., Mesozoic species) being easily recognised as reworked. Consideration was also given to whether a grain was reworked based on the level of thermal maturity and its state of preservation. All palynomorphs identified as in situ are regarded as being penecontemporaneous with deposition and are included in the final calculation of sporomorph percentages. Pollen percentages were plotted using riojaPlot, based on the R package rioja (Juggins, 2020) and local zones were established using the CONISS (Constrained Incremental Sum-of-Squares: Grimm, 1987) cluster analysis function. Sporomorph diversity was measured using both the Shannon–Wiener index and the observed number of taxa. A rarefaction method for sums of ≥ 50 and ≥ 100 grains was applied, so that the effect caused by differences in the sample size may be removed allowing the estimation of the number of sporomorph species at a constant sample size (Raup, 1975; Birks and Line, 1992). The Shannon–Wiener Index was also carried out as the second measure of sporomorph diversity accounting for species richness and evenness (Shannon, 1948; Magurran, 2013; Morris et al., 2014). Samples containing less than 50 grains were omitted from this analysis. Detrended Correspondence Analysis (DCA) was performed, with downweighting of rare species by removing pollen types whose representation is $< 5\%$. This ordination technique is used in order to evaluate ecological patterns within the data, using knowledge of the distribution of NLR and their modern environmental gradients (Correa-Metrio, 2014). Rarefaction, Shannon–Wiener and DCA were all



performed using the software R for statistical computing (R Development Core Team, 2013) and the package Vegan (Oksanen et al., 2013).

100 2.1 Bioclimatic Analysis

Estimates for terrestrial mean annual temperature (MAT), mean annual precipitation (MAP), warmest month mean temperature (WMMT) and coldest month mean temperature (CMMT) were obtained using the NLR approach in conjunction with the Probability Density Function (PDF) method. Fossil taxa used and their NLR are shown in Table 2.

105 Climate estimates based on the NLR approach use presence or absence data and are independent of the relative abundance of individual taxa. This makes this method ideal for sporomorph based climate estimates from marine sediments, where hydrodynamic sorting of grains may cause variations in the percentages of individual taxa (Arias, 2015), and also helps reduce taphonomic biases (Klages et al., 2020). However, the assumption that modern species and their climate requirements are an analogy for the geological past is one of the biggest weaknesses of the NLR approach. This uncertainty inevitably increases
110 the further back in the geological record (Hollis et al., 2019). It should also be noted that the modern distribution of species may be a function of either its past climate or biogeographic history (Reichgelt et al., 2016; Willard et al., 2019). Nevertheless, temperature estimates derived from the NLR approach are often in agreement with those from other botanical methods and geochemical proxies, providing a certain level of confidence (Klages et al., 2020; Pross et al. 2012).

115 The PDF method is used to statistically constrain the most likely climate co-occurrence window for an assemblage (Harbert and Nixon, 2015; Willard et al., 2019; Klages et al., 2020). The bioclimatic envelope for each NLR was identified by cross plotting the modern distribution from the Global Biodiversity Information Facility (GBIF; GBIF, 2021) with the gridded WorldCLIM (Fick and Hijmans, 2017) climate surface data using the dismo package (Hijmans et al., 2017) in R. Some taxa were grouped at the family level because of their potentially ambiguous climatic affinity. This includes (1) taxa belonging to
120 the genus *Nothofagus*, a group that is one of the most abundant in the Antarctic fossil record, due to the ambiguous climatic affinity of the subgenus *Brassospora*, now endemic to New Caledonia; (2) pollen taxa affiliated with the modern-day genus *Microcachrys*, of which *Microcachrys tetragona* is the sole species, on the basis that *M. tetragona* is only found in specific location in Tasmania under narrow climatic and environmental conditions which are likely not representative of this once widespread genus; and (3) the pollen taxa *Peninsulapollis gillii*, which has links to the modern genus *Beauprea* now also
125 endemic to New Caledonia. In these cases, Nothofagaceae, Podocarpaceae and Proteaceae were used, respectively, rather than the genus or species as the NLR.

2.3 Geochemical analyses

The following section will focus on the interpretation of lipid biomarker (*n*-alkane) and stable isotope data from Site 696. For a full description of geochemical methods see López-Quirós et al., in review.



130 2.3.1 Lipid biomarkers (*n*-alkanes)

The distribution of *n*-alkanes in sediments can be assessed on the basis of carbon chain length in order to determine potential biological sources (Cranwell, 1973; Rieley et al., 1991; Bi et al., 2005; Duncan et al., 2019; López-Quirós et al., in review). Algae and bacteria typically produce shorter chain lengths (C₁₂-C₂₂; Clark and Blumer, 1967; Han and Calvin, 1969; Cranwell et al., 1987; Grimalt and Albaigés, 1987; Duncan et al., 2019), while aquatic plants and *Sphagnum* mosses are characterised
135 by enhanced production of C₂₃ to C₂₅ chain lengths (Baas et al., 2000; Ficken et al., 2000; Pancost et al., 2002; Bingham et al., 2010; Duncan et al., 2019). Long chain *n*-alkanes (C₂₅ and higher) are most abundantly produced by terrestrial higher plants (Eglinton and Hamilton, 1963; Duncan et al., 2019). Therefore, medium to long chain *n*-alkane (C₂₃-C₃₁) distributions can provide details about the origin of organic matter in sediments, differentiating between terrigenous and marine, providing information about palaeovegetation and palaeoclimate (Meyers et al., 1997; Ficken et al., 2000; Schefuß et al., 2003; Vogts et al., 2009; Duncan et al., 2019; López-Quirós et al., in review).
140

(a) ACL (Average Chain Length *n*-alkane index)

The ACL index indicates the dominant *n*-alkane in a given carbon number range (Poynter et al., 1989; Schefuß et al., 2003; Duncan et al., 2019) and is calculated following Eq. (1):
145

$$\text{ACL} = \frac{\sum[C_i] \cdot i}{\sum[C_i]}, \quad (1)$$

C_i = carbon number of the odd chain length *n*-alkanes (i.e., from *n*-C₂₅ to *n*-C₃₁).

i = concentration of the odd *n*-alkanes.

Variations in the ACL index through time can be used as a proxy of terrestrial organic matter inputs and can also provide information on changes in climate (Collister et al., 1994; Rommerskirchen et al., 2006; Mahiques et al., 2017; Duncan et al., 2019; López-Quirós et al., in review). Plants produce higher ACLs in warmer, tropical regions, whilst lower ACLs are generally observed from cooler climates (Poynter et al., 1989; Sicre and Peltzer, 2004; Jeng, 2006; Vogts et al., 2009; Bush and McInerney, 2015; Duncan et al., 2019; López-Quirós et al., in review). Studies have also suggested plants synthesise
155 longer *n*-alkanes in more arid environments providing plants with a more efficient wax coating to restrict water loss (e.g., Kolattukudy et al., 1976; Schefuß et al., 2003; Calvo et al., 2004; Zhou et al., 2005; Moossen et al., 2015; Jalali et al., 2017, 2018), indicating aridity has a strong control on ACL and that ACL index values decrease under wetter conditions (Duncan et al., 2019; López-Quirós et al., in review).

160 (b) P_{aq} (Aquatic Plant *n*-alkane index)



The P_{aq} index provides an approximate measure of the relative sedimentary contribution of submerged and floating aquatic macrophytes relative to emergent and terrestrial vegetation (Ficken et al., 2000; López-Quirós et al., in review) and is calculated following Eq. (2):

$$165 \quad P_{aq} = \frac{C_{23}+C_{25}}{C_{23}+C_{25}+C_{29}+C_{31}}, \quad (2)$$

where relationships between n -alkane indices were studied using Pearson's correlation coefficients and assessed as statistically significant when $p < 0.05$.

Sphagnum mosses also have a molecular distribution similar to submerged and floating macrophytes, showing enhanced
170 production of C_{23} and/or C_{25} (Baas et al., 2000; Nott et al. 2000; Nichols et al., 2006; Duncan et al., 2019). Therefore, the P_{aq} index reflects the input from *Sphagnum* and aquatic plants versus terrestrial vegetation. At Site 696 P_{aq} values < 0.23 indicate a dominance of terrestrial plant waxes, while higher values of 0.48 to 0.49 imply an enhanced contribution of enhanced submerged and floating, and/or *Sphagnum* moss (López-Quirós et al., in review).

175 (c) TI (Terrestrial n -alkanes index)

The TI index is based on the assumption that inputs from photosynthetic algae and bacteria are characterised by short-chain n -alkanes (C_{12} - C_{22} ; Clark and Blumer, 1967; Han and Calvin, 1969; Cranwell et al., 1987; Grimalt and Albaigés, 1987; Duncan et al., 2019) compared to higher land plants rich in C_{27} , C_{29} and C_{31} (Bourbonniere and Meyers, 1996; Mahiques et al., 2017;
180 López-Quirós et al., in review). The TI index is calculated as a ratio over the Total Organic Carbon (TOC; Mahiques et al., 2017) following Eq. (3):

$$TI = \frac{\Sigma C_{27+29+31}}{TOC}, \quad (3)$$

This parameter therefore assumes that higher values of TI characterize a greater input of terrestrial plant-derived organic matter (Mahiques et al., 2017; López-Quirós et al., in review).

185 2.3.2 TOC (Total Organic Carbon)

TOC represents the organic fraction preserved in sediments and can be used to help distinguish between marine and terrestrial sources of organic matter, depositional conditions and organic matter production (Calvert and Pedersen, 1993; Meyers and Ishiwatari, 1993; Avramidis et al., 2014, 2015). Organic matter in marine sediments is mainly derived from the decomposition of plants, animals and most importantly plankton (Avramidis et al., 2015). High planktonic primary production and
190 zooplankton grazing causing an increased export of organic matter through the water column to the sea floor support increased preservation of organic carbon in sediments. Therefore, TOC may be used as an indicator for palaeoproductivity even though



195 it also depends on degradation and thus the residence time in the water column (Sarnthein et al. 1988; Lyle et al. 1988; Berger and Herguera 1992; Freudenthal et al. 2002; Jahn et al. 2003; Luo et al., 2013; Frihmat et al., 2015). Coastal sediments with a shorter water column contain higher amounts of TOC than open sea sediments. Organic carbon burial is also affected by redox conditions, and terrigenous detrital matter influx also exert a control and should be taken into account when interpreting TOC in terms of palaeoproductivity (Luo et al., 2013). At Site 696 increased levels of TOC coincide with higher abundance of heterotrophic dinoflagellate cysts (Houben et al., 2013) and may be used to support the notion of high marine palaeoproductivity.

3. Results

200 The recovery of palynomorphs is good throughout the section. Of the 34 samples analysed 5 do not contain a sufficient amount of sporomorphs and were discarded from further analysis. In total 74 pollen taxa (58 angiosperms and 16 gymnosperms), 24 spores and 1 sporomorph of unknown affiliation were identified (excluding reworked and unidentified sporomorphs), containing 54 genera. The stratigraphic distribution and relative abundance of major taxa groups is shown in Fig. 3. Major pollen and spore taxa, in order of decreasing abundance, include *Nothofagidites spp.*, *Podocarpidites spp.*, undifferentiated bisaccates, *Cyathidites spp.*, *Phyllocladidites spp.* and *Retitriletes*, which occur commonly throughout the Eocene and
205 Oligocene sections.

Based on the results of CONISS ordination the succession is divided into 2 main zones (I and II; Fig. 3). In addition, Zone I is further subdivided (Ia Ib), based on the abundance and frequency of taxa. The results of rarefaction and DCA analysis along
210 with the diversity indices results also show a good distinction between Zones I and II.

3.1 Zone I, 37.6-33.6 Ma (643.73-568.82 mbsf)

Zone I comprises of 18 samples (62R 6W 142-144 to 55R 1W 62-64). Based on the age models of Wei and Wise (1990) and Houben et al. (2013, 2019) and linear extrapolation, the lowermost 16 samples are placed in the Eocene, while the uppermost 2 samples are placed into the earliest Oligocene (37.6 Ma to ~33.6 Ma). Quantitatively, Zone I is typified by relatively low
215 numbers of sporomorph species and low diversity. Based on rarefaction analysis, the average number of sporomorph species per sample is 13.28 ± 1.05 (mean \pm SD) at a count of 50 specimens. Low levels of diversity are confirmed by the Shannon diversity indices (H), which indicates an average of 1.79 ± 0.06 .

The overall Zone I assemblage is dominated by the southern beech, *Nothofagus* (pollen taxa: *Nothofagidites*). On average
220 *Nothofagidites* pollen accounts for 79.0% of all non-reworked taxa and 95.0% of all angiosperm taxa. Taxa belonging to the *Nothofagidites lachlaniae* complex (subgenus: *Fuscospora*) are the most abundant followed by undifferentiated *Nothofagus spp.* sporomorphs and taxa belonging to the *N. rocanensis/saraensis* complex (subgenus: *Nothofagus*). Other angiosperm pollen (non-*Nothofagidites*) is rare, making up about 4.2% of the non-reworked sporomorph assemblage in Zone 1. Of the



non-*Nothofagus* angiosperm taxa the most abundantly occurring, in order of decreasing abundance, include *Proteacidites*
225 (NLR: Proteaceae), *Tricolpites* (Dicotyledonae), *Liliacidites intermedius* (Liliaceae) and *Lateropora glabra* (*Freycinetia*).
Other less common angiosperms are typically only represented by one or two occurrences. The second most abundant group
are the gymnosperms, which account for 10.6% of all non-reworked taxa. Predominantly gymnosperms are represented by the
pollen taxa (in order of abundance) *Podocarpidites*, *Phyllocladidites*, *Trichotomosulcites subgranulatus* (all Podocarpaceae)
and *Araucariacites australis* (Araucariaceae). Undifferentiated bisaccate grains also make up a large portion of the
230 gymnosperms observed in Zone I. Many of these are likely to belong to *Podocarpidites* however folding of the grains has
made further identification impossible. Cryptogams account for 6.23% of non-reworked taxa in Zone I and include both ferns
and mosses. Abundantly occurring cryptogam spores include taxa belonging to the *Retitriletes/Lycopodiacidites spp.* complex
(Lycopodiaceae), *Cyathidites* (Cyatheaceae), *Ischyosporites gremius* (Filicopsida) and *Coptospora archangelskyi*
(*Conostomum*).

235

The Subzone Ia assemblage is unique in that *Arecipites spp.* (Arecaceae), *Beaupreaidites* (Beauprea), *Myrtaceidites cf.*
mesonesus (Myrtaceae) and *Dacrydiiumites florinii/praeacupressinoides* (*Dacrydium*), all warmth loving taxa whose NLRs
predominantly have a tropical and subtropical distribution, especially in the Pacific, Southeast Asia and New Caledonia, and
only occur in this subzone. *Ericipites cf. scabratus* (Ericaceae), *Chenopodipollis cf. chenopodiaceoides* (Chenopodiaceae),
240 *Polypodiisporites cf. radiatus* (*Davallia*) and *Podosporites* (Podocarpaceae) are also unique to Subzone Ia of Zone I. In
addition, taxa belonging to the *Nothofagidites asperus* complex (subgenus: *Lophozonia*), *Microcachryidites antarcticus*,
Trichotomosulcites subgranulatus (both Podocarpaceae), *Gleicheniidites* (Gleicheniaceae) and *Ischyosporites* (Filicopsida)
are more abundant than the rest of Zone I. Whereas, *Coptospora* (*Conostomum*) and *Liliacidites* are less abundant than the
remainder of Zone I. Of the entire studied section, *Proteacidites cf. Scabratriporites* greatly increase in abundance and
245 frequency from Subzone Ib. Other rare taxa also only occur in Subzone Ia or Ib of Zone I but are represented by one or two
specimens. Sporomorph-based climate reconstructions reveal significantly higher temperatures within Subzone Ia compared
to Subzone Ib, with an interval of latest Eocene cooling occurring around 35.5 Ma. MAT ranges from 10.9°C to 16.6°C and
MAP ranges from 1418mm to around 1850mm, with an average of 12.8°C and 1661mm respectively for Subzone Ia. For
Subzone Ib MAT ranges from 10.3°C to 11.4°C and MAP is between 1362mm and 1858mm, with an average of 10.8°C and
250 1591mm respectively (Fig. 4).

3.2 Zone II, ca. 33.5-32.2 Ma (563.38-549.70 mbsf)

The 11 samples of Zone II (53R 1W 80-82 to 54R 3W 38-41) are assigned an Oligocene age. Zone II records a strong increase
in gymnosperms and cryptogams, accompanied by a rapid rise in taxa diversity between ca. 33.5 and 32 Ma and a
contemporaneous increase in reworked Mesozoic sporomorphs (Fig. 3). Based on the results of rarefaction analysis the average
255 number of sporomorph species for a count size of 50 individuals is 19.63 ± 2.00 . The results of the Shannon diversity index
are between 1.97 and 2.12, with an average of 2.06 ± 0.05 .



The Zone II sporomorph assemblage shows a significant decrease in *Nothofagus* compared to Zone I. *Nothofagus* pollen make up 51.2% of all non-reworked taxa and 89.9% of all angiosperm taxa in Zone II. Pollen taxa belonging to the *Nothofagidites lachlaniae* complex (subgenus: *Fuscospora*) remain the most abundant, followed by taxa belonging to the *N. rocanensis/saraensis* complex (subgenus: *Nothofagus*), with undifferentiated *Nothofagidites spp.* sporomorphs close behind. However, other *Nothofagus* taxa are less abundant. Although a slight increase in other angiosperms (non-*Nothofagus*) occurs in Zone II they remain the smallest botanical group, representing just 5.8% of all non-reworked sporomorphs. In order of abundance, from least to most abundant, significant non-*Nothofagus* angiosperm taxa include *Proteacidites*, *Tricolpites*, *Myricipites harrisii* (Casuarinaceae) and *Peninsulapollis gillii* (Proteaceae). Additional angiosperm taxa are typically represented by one or two occurrences. Gymnosperms remain the second most abundant botanical group, but their abundance has increased strongly, representing 28.3% of all non-reworked sporomorphs in Zone II. The gymnosperm assemblage remains dominated by *Podocarpidites* and *Phyllocladidites*, which are the two most common gymnosperm taxa respectively. However, other changes in the gymnosperm pollen assemblage are taking place with *Dilwynites (Wollemia)* particularly increasing in frequency and abundance, along with *Alisporites cf. australis* (Gymnospermopsida), *Microcachrydites antarcticus*, *Podosporites* and *Trichotomosulcites subgranulatus* (all Podocarpaceae), among others. Undifferentiated bisaccate grains, that likely belong to *Podocarpidites*, also continue make up a large proportion of the assemblage but are unable to be properly identified. Sporomorph-based climate estimates provide no evidence for abrupt cooling at the Eocene/Oligocene boundary. Within the early Oligocene Zone II MATs are between ~10.3°C to 13.7°C and MAP ranges from 1423mm to 1860mm a year, with an average of 11.5°C and 1626mm respectively (Fig. 4). These results indicate a slight increase in both temperature and precipitation compared to the latest Eocene Subzone Ib.

4. Discussion

4.1 Sediment Transport and Provenance

The late Eocene terrestrial vegetation assemblage from Site 696 shares a number of similarities with Antarctic Peninsula palaeofloras of similar ages (e.g., Warny and Askin 2011b; Warny et al., 2019). Both Site 696 and Antarctic Peninsula late Eocene assemblages are dominated by *Nothofagidites* pollen, predominantly those related to the modern subgenus *Fuscospora*, with secondary gymnosperms including high frequencies of podocarp conifer pollen. Similar angiosperm and cryptogam assemblages are also seen between the two, with angiosperms such as Proteaceae and Liliaceae and cryptogams such as Cyatheaceae and *Sphagnum*. This finding may therefore suggest that pollen from the Antarctic Peninsula region could have been transported to the SOM during this time. Furthermore, similarities between nearby Seymour Island sediments, both in composition and paleogeographic setting, suggest a related source, and that the SOM was proximal enough to receive some detritus from the Antarctic Peninsula (Barker et al., 1988; López-Quirós et al., in review). However, despite these similarities' significant differences in the palaeoflora occurs between the two regions indicating the Antarctic Peninsula may not have been



the primary sediment source. In agreement with previous observations by Mohr (1990) the sporomorph assemblage from Site
290 696 contains a greater diversity of angiosperm pollen compared to late Eocene Antarctic Peninsula palaeofloras (e.g., Anderson
et al., 2011; Warny and Askin 2011b; Warny et al., 2019). This higher diversity has also been reported in southern South
American Paleogene sporomorph floras (e.g., Romero and Zamalao, 1985; Romero and Castro, 1986). In addition, the late
Eocene Zone Ia assemblage (37.6-35.5 Ma) contains the paratropical taxa and warmth loving taxa *Arecipites spp.* (Arecaceae),
Myrtaceidites cf. mesonesus (Myrtaceae), *Dacrydiumites florinii/praecupressinoides* (*Dacrydium*) and *Polypodiisporites cf.*
295 *radiatus* (*Davallia*) not recorded in coeval Antarctic Peninsula assemblages, possibly due to the more northern latitude of the
SOM resulting in milder climatic conditions. In addition, the occurrence of moderate to well-preserved in situ benthic
foraminifera, with predominantly angular to subangular terrigenous particles, does not support the notion of long-distance
transport of sediments from adjacent sources (e.g., Seymour Island; López-Quirós et al., in review). These observations,
together with an expansion of gymnosperm conifers and cryptogams recorded during the early Oligocene (33.5-32.2 Ma) at
300 Site 696, but absent from Antarctic Peninsula floras (e.g., Askin et al., 1992; Anderson et al., 2011), suggest that the vegetation
of the SOM was unique in character and that a significant proportion of detrital material was likely of local origin (e.g., exposed
parts of the SOM).

Furthermore, the SOM and the northern Antarctic Peninsula underwent significant rifting during the late Eocene and early
305 Oligocene (~37-30 Ma; King and Barker, 1988; Eagles and Livermore, 2002; van de Lagemaat et al., 2021), forming what
would become the Powell Basin (Eagles and Livermore, 2002; Eagles and Jokat, 2014; van de Lagemaat et al., 2021; López-
Quirós et al., in review). Throughout the latest Eocene (~35.5–34.1Ma), a decrease in the delivery of coarse terrigenous
sediments and a drop in sedimentation rates by almost half is observed as the SOM became more distal from the Antarctic
Peninsula due to the opening of the proto-Powell Basin (Eagles and Livermore, 2002; López-Quirós et al., in review).
310 Deposition of moderately to intensely bioturbated silty mudstones across the EOT (~34.1–33.6Ma) indicate continued
subsidence-related marine transgression at Site 696 (López-Quirós et al., in review). This subsequent and continued isolation
of the SOM would have caused Site 696 to receive a greater proportion of localised sediments from exposed parts of the SOM.
This supports the results of this study that the majority of sediments supplied to Site 696 at this time were of local origin,
perhaps still with some contribution from the northern Antarctic Peninsula.

315 Conversely however, Carter et al. (2017) suggested the majority of the late Eocene (~36.5–33.6 Ma) sediments deposited at
Site 696 are not of local origin. Using detrital zircon U-Pb and apatite thermochronometry analysis these authors concluded
that sand grains from the late Eocene Site 696 best matched sources within the Ellsworth–Whitmore Mountains in West
Antarctica and that sediments therefore must have been transported to the SOM by ice. However, the presence of in situ
320 paratropical taxa within the early-late Eocene of Site 696 (37.6-35.5 Ma) suggests mild and even ice-free conditions during
this overlapping time period. Furthermore, palaeo-sea-surface temperature reconstructions (Douglas et al., 2014; Hoem and
Bijl, unpublished) indicate relatively warm conditions (~14°C), and fossil dinoflagellate cyst (Houben et al., 2013, 2019),



calcareous nannofossils (Wei and Wise, 1990) and smectite-dominated clay mineralogy (Fig. 2: Robert and Maillot, 1990) support temperate depositional conditions (López-Quirós et al., in review) not favourable for transport by ice. Sediments deposited within two coarse-grained mudstone intervals within a fine-grained transgressive sequence are likely sourced from coastal/shelf areas of the SOM (López-Quirós et al., in review), attesting to the continued supply of detritus from the SOM. Therefore, these results and those of this study indicate that transportation by ice was unlikely and that a majority of sediments transported to Site 696 are likely of local origin from exposed parts of the SOM.

4.2 Palaeoenvironment

4.2.1 Late Eocene Palaeoenvironment

Sediments from Site 696 record two distinct palaeofloras from the late Eocene Zone I to the early Oligocene Zone II assemblage that evolved in response to an increase in environmental disturbance beginning around 34.1 Ma. Throughout the Zone I assemblage (~37.6-33.6 Ma) abundant *Nothofagus* with secondary *Podocarpaceae*, minor angiosperm and cryptogam elements indicate the presence of a relatively humid *Nothofagus*-dominated temperate rainforest, growing under MATs between ~10.3°C and 16.6°C, and MAP of 1362mm and 1858mm (Fig. 4). Comparison with lipid biomarker *n*-alkane results (Fig. 5.; López-Quirós et al., in review) indicates ACL indicative of temperate vegetation, supporting this interpretation. In addition, marine palynomorphs (Houben et al., 2013) and calcareous nannofossil (Wei and Wise, 1990) assemblages attest to temperate marine depositional conditions further suggesting temperate conditions prevailed during this time. *Nothofagus* (predominantly *Fuscospora*-type), together with less common *Podocarpaceae*, formed the forest canopy across much of the mid- to higher-altitude areas, with tracts perhaps dominated by one or the other due to natural differences in shade tolerance (Poole, 1987; Veblen et al., 1996; Gallagher et al., 2008; Bowman et al., 2014). *Microcachrys* along with *Araucariaceae*, *Ericaceae*, *Liliaceae*, *Chenopodiaceae* and low growing proteaceous shrubs, also reflect better drained higher-altitude habitats as well as coastal and marginal forest environments (Kühl et al., 2002; MacPhail et al., 1999; Kershaw and Wagstaff, 2001; Bowman et al., 2014). Today, similar cool temperate *Nothofagus*-dominated mixed-podocarp forests occur in the temperate Valdivian region of southern Chile, between 37°45' and 43°20'S (Veblen et al., 1983, 1996; Poole et al., 2001, 2003; Cantrill and Poole, 2012a; Bowman et al., 2014) across elevations greater than 2000m to lowland areas (Kershaw, 1988; Punyasena et al., 2011; Arias, 2015), where westerly trade winds from the Pacific result in high precipitation.

Pollen taxa representing vegetation communities with very different temperature requirements exist within the early-late Eocene (~35.5-37.6 Ma) Subzone Ia. The presence of the paratropical taxa *Arecaceae* (palms), *Beauprea*, *Myrtaceae* and *Dacrydium*, each occurring intermittently throughout this subzone (643.73-597.66 mbsf), indicates the existence of a temperate-paratropical vegetation community. These communities are not recorded in coeval Antarctic Peninsula assemblages perhaps due to the Antarctic peninsulas high mountainous palaeotopography (Wilson et al., 2012) and/or the lower latitude of the SOM. Paratropical taxa likely occupied sheltered lowland areas and favourable coastal margins and would have required



355 mild temperatures and the absence of winter frosts, owing to the frost sensitivity of extant palms (Larcher and Winter, 1981,
Tomlinson, 2006, Eiserhardt et al., 2011, Reichgelt et al., 2018). Sporomorph based climate estimates reveal Coldest Month
Mean Temperatures (CMMT) between 7.5°C and 13.5°C, well above freezing (Fig. 4). In addition, warmth-loving ferns
including Gleicheniaceae and rare Davalliaceae also occur together with moisture-loving conifers such as *Dacrydium*, which
only occur in Subzone Ia, and *Phyllocladus*, further indicating warm wet temperate conditions throughout this subzone. Today
360 these taxa occur in subtropical to temperate regions in lowland sheltered environments, often thriving in wet humid conditions
and severely disturbed or pioneer habitats at the margins of rainforests and waterways (Specht et al., 1992; Chinnock and Bell,
1998; Bowman et al., 2014; Arias, 2015).

The co-occurrence of prominent vegetation communities, each with very different temperature and moisture requirements
365 therefore suggests that late Eocene forests across the northern Antarctic Peninsula and SOM were subject to climatic gradients
related to differences in elevation and proximity to the coastline. Furthermore, the presence of paratropical and warm taxa
within Subzone Ia and the lack of cold temperature taxa reveal conditions were warmer, by around 2°C between 37.6 and 35.5
Ma, compared to the rest of Zone I and the early Oligocene Zone II, indicating a phase of latest Eocene cooling from 35.5 to
35 Ma. The cooling between 35.5 and 35 Ma recorded by the terrestrial palynomorph assemblage coincides with a slight
370 decrease in the terrestrial *n*-alkanes Index (TI; Mahiques et al., 2017), which records absolute input of *n*-C₂₇₊₂₉₊₃₀-rich
molecules present in vascular plants, indicating decreased input of terrestrial plant-derived organic matter (Fig. 5; López-
Quirós et al., in review). The latest Eocene cooling recorded at Site 696 after 35.5 Ma corresponds with large-scale changes in
vegetation composition and decreasing diversity from Antarctic Peninsula palaeoflora records (e.g., Askin, 2000; Anderson et
al., 2011; Warny and Askin, 2011a, 2011b). Furthermore, an upwards-increase in illite clay minerals (Robert and Maillot,
375 1990) between approximately 36.4 to 33.9 Ma, signifying a shift in weathering regime from chemical to physical, supports the
idea of latest Eocene climate cooling.

An initial spike in reworked Mesozoic sporomorphs at around 34.1 Ma at the onset of the EOT indicates an increase in
reworking. This coincides with increasing Eocene dinoflagellate cyst taxa percentages over Protoperidiniaceae (Houben et al.,
380 2013). Sediments within this EOT interval also exhibit two coarsening-upward packages, within an otherwise fine-grained
sequence. Furthermore, these sedimentary packages contain the first evidence for ice-rafted debris (IRDs; Barker et al., 1988;
López-Quirós et al., in review) in conjunction with a high percentage of illite clay minerals (Robert and Maillot, 1990). Based
on these observations, significant ice build-up around the northern Antarctic Peninsula and SOM is inferred, with a period of
continental ice expansion to the coast or beyond (López-Quirós et al., in review). This is supported by the presence of glacial
385 surface textures on sand grains (Kirshner and Anderson, 2011) and rare drop stones (Wellner et al., 2011) from late Eocene
(34-37 Ma; Bohaty et al., 2011) sediments offshore James Ross Basin, as well as other sedimentological and geochemical
evidence indicating late Eocene and early Oligocene cooling and ice expansion on the northern Antarctic Peninsula (e.g.,
Robert and Maillot, 1990; Ivany et al., 2008). Furthermore, topographic reconstructions indicate the northern Antarctic



390 Peninsula at the EOT was comparable in elevation to the Trans Antarctic Mountains and Dronning Maud Land (Wilson et al., 2012). In model simulations these are suggested nucleation points for late Eocene and Oligocene glaciation (DeConto and Pollard 2003; DeConto et al., 2007), suggesting a glacial presence in the Antarctic Peninsula region is reasonable during this time (Carter et al., 2017; Lepp, 2018). However, the pollen and spore assemblage from site 696 as well as other late Eocene and Oligocene sporomorph assemblages from the Antarctic Peninsula (e.g., Anderson et al., 2011; Askin and Warny 2011a), indicate the region still retained some vegetation and therefore was never fully glaciated.

395 4.2.2 Early Oligocene Palaeoenvironment

Despite the evidence for a cooling of terrestrial climate between 35.5 Ma and 35 Ma, and latest Eocene glacial onset around 34.1 Ma the terrestrial palynomorph assemblage from Site 696 indicates that *Nothofagus*-dominated forests did not change dramatically in composition until the early Oligocene, after the EOIS. An expansion of conifer trees and cryptogams accompanied by a rapid increase in taxa diversity is recorded between approximately 33.5 and 32 Ma. This significant transformation of Antarctic flora in the early Oligocene is quantitatively reflected by the results of DCA analysis, as well as by a decrease in *n*-alkane ACL, which in turn suggest herbaceous plants and/or conifer dominance (Fig. 5; López-Quirós et al., in review). The diversity patterns derived from the Shannon diversity index and rarefaction analysis show that early Oligocene forests contained a significantly higher number of taxa compared with the late Eocene forest communities. Previous studies (e.g., Cantrill, 2001; Rain and Askin, 2001; Prebble et al., 2006; Griener and Warny, 2015) suggest that significant cooling and drying of the climate across the EOT led to decreasing diversity and a lowering of the forest canopy, with low stature forests formed of scrubby dwarf *Nothofagus* and podocarps in sheltered regions and low altitude coastal zones. However, based on the relatively high diversity and frequency of cryptogam taxa and non-*Nothofagus* angiosperms within the Zone II assemblage, these *Nothofagus*-podocarp forests would have been at least intermediate in stature and relatively open, allowing the development of fern, shrub and bryophyte communities (e.g., Macphail and Truswell, 2004). When compared to *n*-alkane results an increase in the abundance of cryptogams, specifically *Sphagnum* moss, is also supported by an increase in the aquatic plant *n*-alkane index (P_{aq}) and $n-C_{23}/n-C_{29}$ ratios throughout the early Oligocene (López-Quirós et al., in review).

Within the early Oligocene (~33.5-32.2 Ma) Zone II assemblage, the increase in *Coptospora* and *Stereisporites* (*Sphagnum*), along with some angiosperms such as *Liliacidites* and possibly *Myricipites*, suggest the progression towards colder environments. *Coptospora* and *Liliacidites* have been found in Oligocene and Miocene assemblages across Antarctica, including the Ross Sea region (e.g., Askin and Rain, 2000; Prebble et al., 2006), Meyer Desert Formation (e.g., Lewis et al., 2008), Wilkes Land (e.g., Sangiorgi et al., 2018) and the Antarctic Peninsula (e.g., Warny and Askin 2011a). These Oligocene/Miocene assemblages have been inferred to represent tundra mosaic vegetation in cold, possibly glacial, landscapes (Francis and Hill, 1996; Macphail and Truswell, 2004; Prebble et al., 2006). In addition, the presence of common millimetre sized IRDs between approximately 564 and 560 mbsf suggests phases of continental ice expansion to coastal and possibly shelf areas (Barker et al., 1988; López-Quirós et al., in review). Within this same interval sporomorph-based climate



reconstructions also reveal a cooling and drying step, with a decrease in MAT and MAP from around 13.4°C to 10.7°C and 1815mm to 1423mm, between ~33.5 Ma and 33.4 Ma. The initially relatively high temperatures during the earliest Oligocene may be associated with the reported return to near-Eocene climate soon after the EOT (Liu et al., 2009; Houben et al., 2012; 425 Wilson et al., 2013) and is possibly also reflected in a shift in some organic matter indices across the EOT and after the EOIS (Fig. 5; López-Quirós et al., in review). However, further interpretation of this sediment section is hampered by a gap in core recovery. The increase in typical tundra taxa together with common IRD indicates a potential phase of cooling and glacial expansion during the earliest Oligocene, possibly punctuated by the development of milder climates (e.g., Liu et al., 2009; Houben et al., 2012; Wilson et al., 2013).

430

Warming and cooling phases with episodes of ice growth and retreat would have caused environmental disturbance, likely reducing the extent of *Nothofagus*-dominated forested areas that were established throughout the Eocene. In New Zealand today *Nothofagus* seedlings are able to capitalise more readily on small canopy openings enabling them to out-compete podocarps in old-growth stands (Lusk et al., 2015). However, unlike podocarps juvenile *Nothofagus* also require shelter from 435 frost and desiccation, finding it hard to establish themselves amongst other vegetation in open and marginal forest environments until this other vegetation has been partially suppressed through overtopping by *Nothofagus* (Wardle, 1964; Lusk et al., 2015 Rawlence et al., 2020). Thus, conifers are probably favoured by exogenous disturbance, providing a short-lived reprieve from angiosperm competition (Enright & Hill 1995; Lusk et al., 2015). Across the EOT and earliest Oligocene glacial related environmental disturbance and the development of milder climates, possibly after the EOT (e.g., Liu et al., 440 2009; Houben et al., 2012; Wilson et al., 2013), would have therefore facilitated the expansion of different vegetation types previously suppressed by the dominance of *Nothofagus*, due to the limited dispersal ability of *Nothofagus*. Furthermore, a study by Galeotti et al. (2016), suggested that until ca. 32.2 Ma any Antarctic ice sheet would have been extremely sensitive to orbitally paced, local insolation forcing and would have been prone to large fluctuations. Variability in ice volume during the early Oligocene are also reflected by greatly varying benthic $\delta^{18}\text{O}$ confirming large fluxes in Antarctic ice during this time. 445 Therefore, the unusual expansion of gymnosperms and cryptogams seen at Site 696 is suggested to be related to an increase in environmental disturbance caused by repeated glacial expansion and retreat, with the first major glacial expansion around 34.1 Ma, together with the competitive dominance of podocarps on exposed disturbed sites (Fig. 6). A lack of evidence for marine reworking after the EOT and good agreement between terrestrial biomarkers (López-Quirós et al., in review) and the fossil sporomorph record suggest that the changes in the terrestrial palynomorph 450 assemblage during the early Oligocene (~33.5 Ma) reflect true climate signals and increased environmental disturbance caused by glacial onset. Moreover, the results of this study reveal that major changes in terrestrial vegetation took place after the onset of glaciation rather than after terrestrial climate cooling that took place during the latest Eocene after 35.5Ma.



4.3 Paleooceanography

455 At the same time as terrestrial cooling at 35.5 Ma, indicated by the loss of paratropical taxa and a decrease in sporomorph-
based MAT estimates, sharp changes to marine environments at site 696 are signalled by the appearance of glauconitic
packstone (~588.8 to 577.9 mbsf; López-Quirós et al., 2019). The formation of this mature glaucony-bearing facies is
suggested to be related to a decrease in the delivery of terrigenous sediments to Site 696 and suboxic reducing conditions at
the sediment water interface (López-Quirós et al., 2019, in review). This change in oceanic environmental conditions may be
460 explained by the opening of the proto-Powell Basin and changes to ocean currents, with several studies (e.g., Lawver and
Gahagan, 1998; Eagles and Livermore, 2002; Livermore et al., 2007) indicating strengthening of Scotia Sea and the northern
Weddell Sea circulation at this time (López-Quirós et al., in review). Decreased terrigenous sediment supply, as the SOM
moved away from the Antarctic Peninsula, is supported by a drop in sedimentation from ~4 cm/kyr between 645.6 to ~597.2
mbsf to ~1.85 cm/kyr between ~588.8 to 577.9 mbsf (López-Quirós et al., 2019, in review). The opening of the Powell Basin
465 to shallow and possibly intermediate waters is also suggested to have resulted in the creation of an upwelling system fuelling
high sea-surface primary productivity and the development of oxygen-deficient bottom waters (López-Quirós et al., in review).
Condensed glauconitic sections on outer shelf-upper slope setting commonly occur beneath upwelling areas with high
productivity (e.g., Cook and Marshall, 1981; Wigley and Compton, 2006; Banerjee et al., 2016). Fe-enrichment of glaucony
grains is likely the result of high sea-surface productivity as a result of upwelling along the margin of the SOM (López-Quirós
470 et al., 2019, in review). Further evidence for increased marine biological productivity at Site 696 comes from distribution
patterns of dinocysts and the proliferation in heterotrophic Protoperidiniaceae dinoflagellates, notably with increased
abundances of the genera *Brigantedinium spp.*, at approximately 34.5 Ma (Fig. 5; Houben et al., 2013, 2019). The dominance
of Protoperidiniaceae dinoflagellates throughout the late Eocene-early Oligocene at Site 696 suggesting eutrophic surface
waters supports the hypothesis of high sea-surface productivity enhanced by upwelling related to the opening of the Powell
475 Basin at 35.5 Ma. Furthermore, high TOC within the early Oligocene combined with the presence of pyrite and diagenetic
barite provide further evidence suggesting high marine productivity, leading to low oxygen conditions at the seafloor, possibly
due to upwelling (López-Quirós et al., in review).

Importantly these change in oceanographic conditions associated with the opening of the Powell Basin occur synchronously
480 with terrestrial cooling at 35.5 Ma, within the resolution of this study. Furthermore, large-scale changes in vegetation
composition and decreasing diversity from Antarctic Peninsula (e.g., Askin, 2000; Anderson et al., 2011; Warny and Askin,
2011a, 2011b) also occur at this time. Therefore, this may suggest a link between marine and terrestrial environments and that
the opening of the Powell Basin and the establishment of oceanic upwelling may have driven a large-scale regional cooling
step at 35.5 Ma. However, the regional change in oceanography and marine environments cannot be directly linked with the
485 terrestrial vegetation change and glacial onset in the region, that took place about one million years later, at 34.1 Ma. The
timing of the second cooling rather suggest that the event at site 696 is linked to the global cooling at the onset of the EOT



which is documented by a combination of deep-ocean cooling and global ice sheet growth marking the step from a largely ice-free greenhouse world to an icehouse climate (Hutchinson et al. 2020).

490 5. Conclusion

The terrestrial palynomorph assemblage from ODP Site 696 in the Weddell Sea records two distinct palaeofloras that evolved in response to increased environmental disturbance and provide insight into late Eocene and early Oligocene terrestrial climate and cryosphere evolution. Late Eocene pollen and spore assemblages reveal a terrestrial climate cooling at 35.5 Ma with a decrease in MAT by an average of 2°C, associated with a shift from temperate-paratropical *Nothofagus*-dominated forests to cool temperate *Nothofagus*-dominated forests. This cooling of terrestrial climate after 35.5 Ma coincides with changes in floral diversity and composition in palaeoflora records from the Antarctic Peninsula (e.g., Askin, 2000; Anderson et al., 2011; Warny and Askin, 2011a, 2011b), which have been interpreted to reflect the onset of prolonged cooling in the region. Despite evidence for terrestrial cooling and ice expansion, *Nothofagus*-dominated forests did not change dramatically in composition until the early Oligocene, when there was distinct expansion of gymnosperms and cryptogams accompanied by a rapid increase in taxa diversity between approximately 33.5 and 32 Ma. We suggest that glacial related environmental disturbance, starting around 34.1 Ma, reflected by an increase in cold climate taxa and sedimentological evidence for ice transport and erosion (e.g., Robert and Maillot, 1990; López-Quirós et al., 2019, in review), facilitated the expansion of different vegetation types previously suppressed by the dominance of *Nothofagus*.

The cooling step at 35.5 Ma coincides with an abrupt change to marine environments at Site 696, indicated by the appearance of mature glaucony-bearing facies (~588.8 to 577.9 mbsf; López-Quirós et al., 2019). Development of this glauconitic section has been related to the opening of the Powell Basin, resulting in decreased sedimentation rates and the development of oceanic upwelling fuelling high marine biological productivity and the development suboxic bottom waters (López-Quirós et al., 2019, in review). The coincidence between terrestrial cooling and changes to ocean currents and marine environments at Site 696 possibly indicates a strong link between ocean and terrestrial environmental change, suggesting the opening of the Powell Basin and reorganisation of ocean currents triggered a regional cooling step at 35.5 Ma prior to glacial onset at 34.1 Ma. However, the large temporal gap (~1.4 Ma) between oceanographic changes and glacial onset suggests that the opening of ocean gateways did not alone trigger glaciation, even if ocean gateways may have played a role in stepwise cooling.



Data Availability

515 All data will be available on the www.pangaea.de database (submitted 02/07/2021, awaiting validation)

Acknowledgments

NT received funding from the Natural Environment Research Council (NERC)-funded Doctoral Training Partnership ONE Planet [NE/S007512/1]. Funding for this research was also provided by the Spanish Ministry of Science and Innovation (grants 520 CTM2014-60451-C2-1/2-P and CTM2017-89711-C2-1/2-P) cofunded by the European Union through FEDER funds. This work used Deep Sea Drilling Project archived samples provided by the International Ocean Discovery Program (IODP). We thank the staff at the Gulf Coast core repository (GCR) for assistance in ODP Leg 113 core handling and shipping. We thank CNRS for the salary support of MAS.

Author contributions

525 NT and US designed the research and NT analysed pollen and spores. ALQ added sedimentological and geochemical analyses. NT prepared the manuscript with contribution from all co-authors.

References

- Anderson, J. B., Warny, S., Askin, R. A., Wellner, J. S., Bohaty, S. M., Kirshner, A. E., Livsey, D. N., Simms, A. R., Smith, T. R., Ehrmann, W., Lawver, L. A., Barbeau, D., Wise, S. W., Kulhanek, D. K., Weaver, F. M., and Majewski, W.: Progressive Cenozoic cooling and the demise of Antarctica's last refugium, *Proc. Natl. Acad. Sci.*, 108, 11356–11360, <https://doi.org/10.1073/pnas.1014885108>, 2011.
- Arias, L. C.: Terrestrial ecosystems on a Greenhouse Earth: Climate and vegetation in the high southern latitudes during the early Paleogene, Ph.D. thesis, Faculty of Geosciences and Geography, Johann Wolfgang Goethe University Frankfurt am Main, Germany, 2015.
- 535 Askin, R. A. and Raine, J. I.: Oligocene and Early Miocene terrestrial palynology of the Cape Roberts Drillhole CRP-2/2A, Victoria Land Basin, Antarctica, *Terra Antart.*, 7(4), 493–501, 2000.
- Askin, R. A.: Spores and Pollen from the McMurdo Sound Erratics, Antarctica, in: *Paleobiology and Paleoenvironments of Eocene Rocks: McMurdo Sound, East Antarctica*, 76, edited by: Stilwell, J. D., Feldmann, R. M., American Geophysical Union, United States, 161-181, <https://doi.org/10.1029/AR076p0161>, 2000.
- 540 Avramidis, P., Iliopoulos, G., Panagiotaras, D., Papoulis, D., Lambropoulou, P., Kontopoulos, N., Siavalas, G., and Christanis, K.: Tracking Mid- to Late Holocene depositional environments by applying sedimentological, palaeontological and geochemical proxies, Amvrakikos coastal lagoon sediments, Western Greece, Mediterranean Sea, *Quat. Int.*, 332, 19–36, <https://doi.org/10.1016/j.quaint.2013.09.006>, 2014.



- Avramidis, P., Nikolaou, K., and Bekiari, V.: Total Organic Carbon and Total Nitrogen in Sediments and Soils: A Comparison
545 of the Wet Oxidation – Titration Method with the Combustion-infrared Method, *Agric. Agric. Sci. Procedia*, 4, 425–
430, <https://doi.org/10.1016/j.aaspro.2015.03.048>, 2015.
- Baas, M., Pancost, R., van Geel, B., and Sinninghe Damsté, J. S.: A comparative study of lipids in Sphagnum species, *Org.
Geochem.*, 31, 535–541, [https://doi.org/10.1016/S0146-6380\(00\)00037-1](https://doi.org/10.1016/S0146-6380(00)00037-1), 2000.
- Banerjee, S., Bansal, U., Pande, K., and Meena, S. S.: Compositional variability of glauconites within the Upper Cretaceous
550 Karai Shale Formation, Cauvery Basin, India: implications for evaluation of stratigraphic condensation, *Sediment.
Geol.*, 331, 12–29, <https://doi.org/10.1016/j.sedgeo.2015.10.012>, 2016.
- Barker, P.F., Kennett, J.P. and Shipboard Scientific Party.: Leg 113, in: *Proceedings of the Ocean Drilling Program Initial
Reports of Leg 113*, 607–704, <https://doi.org/10.2973/odp.proc.ir.113.1900>, 1988.
- Basak, C. and Martin, E. E.: Antarctic weathering and carbonate compensation at the Eocene–Oligocene transition, *Nat.
555 Geosci.*, 6(2), 121–124, <https://doi.org/10.1038/ngeo1707>, 2013.
- Berger, W. H. and Herguera, J. C.: *Reading the Sedimentary Record of the Ocean’s Productivity BT- Primary Productivity
and Biogeochemical Cycles in the Sea*, edited by: Falkowski, P. G., Woodhead, A. D., and Vivirito, K., Springer US,
Boston, MA, 455–486, https://doi.org/10.1007/978-1-4899-0762-2_24, 1992.
- Bi, X., Sheng, G., Liu, X., Li, C., and Fu, J.: Molecular and carbon and hydrogen isotopic composition of n-alkanes in plant
560 leaf waxes, *Org. Geochem.*, 36(10), 1405–1417, <https://doi.org/10.1016/j.orggeochem.2005.06.001>, 2005.
- Bingham, E. M., McClymont, E. L., Väiliranta, M., Mauquoy, D., Roberts, Z., Chambers, F. M., Pancost, R. D., and Evershed,
R. P.: Conservative composition of n-alkane biomarkers in Sphagnum species: Implications for palaeoclimate
reconstruction in ombrotrophic peat bogs, *Org. Geochem.*, 41(2), 214–220,
<https://doi.org/10.1016/j.orggeochem.2009.06.010>, 2010.
- 565 Birks, H. J. B. and Line, J. M.: The use of Rarefaction Analysis for Estimating Palynological Richness from Quaternary Pollen-
Analytical Data, 2(1), 1–10, <https://doi.org/10.1177/095968369200200101>, 1992.
- Bohaty, S. M., Kulhanek, D. K., Wise Jr., S. W., Jemison, K., Warny, S., and Sjunneskog, C.: Age Assessment of Eocene–
Pliocene Drill Cores Recovered During the SHALDRIL II Expedition, Antarctic Peninsula,
<https://doi.org/10.1029/2010SP001049>, 1 January 2011.
- 570 Bourbonniere, R. A. and Meyers, P. A.: Characterization of sedimentary humic matter by alkaline hydrolysis, *Org. Geochem.*,
5(3), 131–142, [https://doi.org/https://doi.org/10.1016/0146-6380\(83\)90023-2](https://doi.org/https://doi.org/10.1016/0146-6380(83)90023-2), 1983.
- Bowman, V. C., Francis, J. E., Askin, R. A., Riding, J. B., and Swindles, G. T.: Latest Cretaceous–earliest Paleogene vegetation
and climate change at the high southern latitudes: palynological evidence from Seymour Island, Antarctic Peninsula,
Palaeogeogr. Palaeoclimatol. Palaeoecol., 408, 26–47, <https://doi.org/10.1016/j.palaeo.2014.04.018>, 2014.
- 575 Bush, R. T. and McInerney, F. A.: Leaf wax n-alkane distributions in and across modern plants: Implications for paleoecology
and chemotaxonomy, *Geochim. Cosmochim. Acta*, 117, 161–179, <https://doi.org/10.1016/j.gca.2013.04.016>, 2013.



- Bush, R. T. and McNerney, F. A.: Influence of temperature and C4 abundance on n-alkane chain length distributions across the central USA, *Org. Geochem.*, 79, 65–73, <https://doi.org/10.1016/j.orggeochem.2014.12.003>, 2015.
- Calvert, S. E. and Pedersen, T. F.: Geochemistry of Recent oxic and anoxic marine sediments: Implications for the geological record, *Mar. Geol.*, 113(1), 67–88, [https://doi.org/10.1016/0025-3227\(93\)90150-T](https://doi.org/10.1016/0025-3227(93)90150-T), 1993.
- Calvo, E., Pelejero, C., Logan, G. A., and De Deckker, P.: Dust-induced changes in phytoplankton composition in the Tasman Sea during the last four glacial cycles, *Paleoceanography*, 19(2), <https://doi.org/10.1029/2003PA000992>, 2004.
- Cantrill, D. J.: Early Oligocene *Nothofagus* from CRP-3, Antarctica: Implications for the vegetation history, *Terra Antart.*, 8(4), 401–406, 2001.
- 585 Cantrill, D. J. and Poole, I.: After the heat: late Eocene to Pliocene climatic cooling and modification of the Antarctic vegetation, in: *The Vegetation of Antarctica through Geological Time*, edited by Cantrill, D. J. and Poole, I., Cambridge University Press, Cambridge, 390–457, [https://doi.org/DOI: 10.1017/CBO9781139024990.009](https://doi.org/DOI:10.1017/CBO9781139024990.009), 2012b.
- Cantrill, D. J. and Poole, I.: The heat is on: Paleogene floras and the Paleocene–Eocene warm period, in: *The Vegetation of Antarctica through Geological Time*, edited by: Cantrill, D. J. and Poole, I., Cambridge University Press, Cambridge, 590 308–389, [https://doi.org/DOI: 10.1017/CBO9781139024990.008](https://doi.org/DOI:10.1017/CBO9781139024990.008), 2012a.
- Carter, A., Riley, T. R., Hillenbrand, C.-D., and Rittner, M.: Widespread Antarctic glaciation during the Late Eocene, *Earth Planet. Sci. Lett.*, 458, 49–57, <https://doi.org/10.1016/j.epsl.2016.10.045>, 2017.
- Chinnock, R. J. and Bell, G. H.: *Gleicheniaceae, flora of Australia Online*, 1998.
- Clark R. C., J. and Blumer, M.: Distribution of n-paraffins in marine organisms and sediment 1, *Limnol. Oceanogr.*, 12, 79–595 87, <https://doi.org/10.4319/lo.1967.12.1.0079>, 1967.
- Collister, J. W., Rieley, G., Stern, B., Eglinton, G., and Fry, B.: Compound-specific $\delta^{13}\text{C}$ analyses of leaf lipids from plants with differing carbon dioxide metabolisms, *Org. Geochem.*, 21(6), 619–627, [https://doi.org/10.1016/0146-6380\(94\)90008-6](https://doi.org/10.1016/0146-6380(94)90008-6), 1994.
- Cook, P. J. and Marshall, J. F.: Geochemistry of iron and phosphorus-rich nodules from the east Australian continental shelf, 600 *Mar. Geol.*, 41(3-4), 205–221, [https://doi.org/10.1016/0025-3227\(81\)90081-5](https://doi.org/10.1016/0025-3227(81)90081-5)1981.
- Cookson, I.: Fossil pollen grains of proteaceous type from Tertiary deposits in Australia, *Aust. J. Biol. Sci.*, 3(2), 166–177, <https://doi.org/10.1071/BI9500166>, 1950.
- Cookson, I. C. and Pike, K. M.: Some dicotyledonous pollen types from Cainozoic deposits in the Australian region, *Aust. J. Bot.*, 2(2), 197–219, <https://doi.org/10.1071/BT9540197>, 1954.
- 605 Correa-Metrio, A., Dechnik, Y., Lozano-García, S., and Caballero, M.: Detrended correspondence analysis: A useful tool to quantify ecological changes from fossil data sets, *Boletín la Soc. Geológica Mex.*, 66(1), 135–143, 2014.
- Coxall, H. K. and Pearson, P. N.: The Eocene-Oligocene transition, *Deep Time Perspect. Clim. Chang. Marrying Signal From Comput. Model. Biol. Proxies*, 351–387, <https://doi.org/10.1144/TMS002.16>, 2007.
- Cranwell, P. A.: Chain-length distribution of n-alkanes from lake sediments in relation to post-glacial environmental change, 610 *Freshw. Biol.*, 3(3), 259–265, <https://doi.org/10.1111/j.1365-2427.1973.tb00921.x>, 1973.



- Cranwell, P. A., Eglinton, G., and Robinson, N.: Lipids of aquatic organisms as potential contributors to lacustrine sediments—II, *Org. Geochem.*, 11, 513–527, [https://doi.org/10.1016/0146-6380\(87\)90007-6](https://doi.org/10.1016/0146-6380(87)90007-6), 1987.
- DeConto, R. M. and Pollard, D.: Rapid Cenozoic glaciation of Antarctica induced by declining atmospheric CO₂, *Nature*, 421(6920), 245–249, <https://doi.org/10.1038/nature01290>, 2003.
- 615 DeConto, R., Pollard, D., and Harwood, D.: Sea ice feedback and Cenozoic evolution of Antarctic climate and ice sheets, *Paleoceanography*, 22(3), <https://doi.org/10.1029/2006PA001350>, 2007.
- Dettmann, M. E., Pocknall, D. T., Romero, E. J., and Zamalao, M. del C.: *Nothofagidites Erdtman ex Potonié, 1960; a catalogue of species with notes on the paleogeographic distribution of Nothofagus Bl. (Southern Beech), New Zeal. Geol. Surv. Paleontol. Bull.*, 1990.
- 620 Dettmann, M. E. and Jarzen, D. M.: Pollen of proteaceous-type from latest Cretaceous sediments, southeastern Australia, 20(2), 103–160, <https://doi.org/10.1080/03115519608619193>, 1996.
- Diekmann, B., Kuhn, G., Gersonde, R., and Mackensen, A.: Middle Eocene to early Miocene environmental changes in the sub-Antarctic Southern Ocean: evidence from biogenic and terrigenous depositional patterns at ODP Site 1090, *Glob. Planet. Change*, 40(3-4), 295–313, <https://doi.org/10.1016/j.gloplacha.2003.09.001>, 2004.
- 625 Dodson, J. R.: Modern pollen spectra from Chatham Island, New Zealand, *New Zeal. J. Bot.*, 14 (4), 341–347, <https://doi.org/10.1080/0028825X.1976.10428907>, 1976.
- Douglas, P. M. J., Affek, H. P., Ivany, L. C., Houben, A. J. P., Sijp, W. P., Sluijs, A., Schouten, S., and Pagani, M.: Pronounced zonal heterogeneity in Eocene southern high-latitude sea surface temperatures, 111(18), 6582–6587, <https://doi.org/10.1073/pnas.1321441111>, 2014.
- 630 Duncan, B., McKay, R., Bendle, J., Naish, T., Inglis, G. N., Moossen, H., Levy, R., Ventura, G. T., Lewis, A., and Chamberlain, B.: Lipid biomarker distributions in Oligocene and Miocene sediments from the Ross Sea region, Antarctica: Implications for use of biomarker proxies in glacially-influenced settings, *Palaeogeogr. Palaeoclimatol. Palaeoecol.*, 516, 71–89, <https://doi.org/10.1016/j.palaeo.2018.11.028>, 2019.
- Eagles, G. and Jokat, W.: Tectonic reconstructions for paleobathymetry in Drake Passage, 611, 28–50, <https://doi.org/10.1016/j.tecto.2013.11.021>, 2014.
- 635 Eagles, G. and Livermore, R. A.: Opening history of Powell Basin, Antarctic Peninsula, *Mar. Geol.*, 185(3-4), 195–205, [https://doi.org/10.1016/S0025-3227\(02\)00191-3](https://doi.org/10.1016/S0025-3227(02)00191-3), 2002.
- Eiserhardt, W. L., Svenning, J.-C., Kissling, W. D., and Balslev, H.: Geographical ecology of the palms (Arecaceae): determinants of diversity and distributions across spatial scales, *Ann. Bot.*, 108, 1391–1416, <https://doi.org/10.1093/aob/mcr146>, 2011.
- 640 El Frihmat, Y., Hebbeln, D., Jaaidi, E. L. B., and Mhammedi, N.: Reconstruction of productivity signal and deep-water conditions in Moroccan Atlantic margin (~35°N) from the last glacial to the Holocene, *Springerplus*, 4(1), 69, <https://doi.org/10.1186/s40064-015-0853-6>, 2015.



- 645 Elliot, D. H.: Tectonic setting and evolution of the James Ross Basin, northern Antarctic Peninsula, in: *Geology and Paleontology of Seymour Island, Antarctic Peninsula*, edited by: Feldmann, R. M., and Woodburne, M. O., Geological Society of America, Memoir no. 16, Boulder, Colorado, 541–555, 1988.
- Enright, N.J. and Hill, R.S. (Eds): *Ecology of the southern conifers*, Melbourne University Press, Carlton, Australia, 1995.
- 650 Feakins, S. J., Peters, T., Wu, M. S., Shenkin, A., Salinas, N., Girardin, C. A. J., Bentley, L. P., Blonder, B., Enquist, B. J., Martin, R. E., Asner, G. P., and Malhi, Y.: Production of leaf wax n-alkanes across a tropical forest elevation transect, *Org. Geochem.*, 100, 89–100, <https://doi.org/10.1016/j.orggeochem.2016.07.004>, 2016.
- Fick, S. E. and Hijmans, R. J.: WorldClim 2: new 1-km spatial resolution climate surfaces for global land areas, *Int. J. Climatol.*, 37(12), 4302–4315, <https://doi.org/10.1002/joc.5086>, 2017.
- 655 Ficken, K. J., Li, B., Swain, D. L., and Eglinton, G.: An n-alkane proxy for the sedimentary input of submerged/floating freshwater aquatic macrophytes, *Org. Geochem.*, 31(7), 745–749, [https://doi.org/10.1016/S0146-6380\(00\)00081-4](https://doi.org/10.1016/S0146-6380(00)00081-4), 2000.
- Francis, J. E. and Hill, R. S.: Fossil plants from the Pliocene Sirius Group, Transantarctic Mountains; evidence for climate from growth rings and fossil leaves, *Palaios*, 11(4), 389–396, <https://doi.org/10.2307/3515248>, 1996.
- 660 Freudenthal, T., Meggers, H., Henderiks, J., Kuhlmann, H., Moreno, A., and Wefer, G.: Upwelling intensity and filament activity off Morocco during the last 250,000 years, *Deep Sea Res. Part II Top. Stud. Oceanogr.*, 49(17), 3655–3674, [https://doi.org/10.1016/S0967-0645\(02\)00101-7](https://doi.org/10.1016/S0967-0645(02)00101-7), 2002.
- Galeotti, S., DeConto, R., Naish, T., Stocchi, P., Florindo, F., Pagani, M., Barrett, P., Bohaty, S. M., Lanci, L., Pollard, D., Sandroni, S., Talarico, F. M., and Zachos, J. C.: Antarctic Ice Sheet variability across the Eocene-Oligocene boundary climate transition, *Science*, 352(6281), 76 LP – 80, <https://doi.org/10.1126/science.aab0669>, 2016.
- 665 Gallagher, S. J., Wagstaff, B. E., Baird, J. G., Wallace, M. W., and Li, C. L.: Southern high latitude climate variability in the Late Cretaceous greenhouse world, *Glob. Planet. Change*, 60(3), 351–364, <https://doi.org/10.1016/j.gloplacha.2007.04.001>, 2008.
- GBIF: GBIF Occurrence Download [data set], <https://doi.org/10.15468/dl.te8pxs>, 2021.
- Gersonde, R., Burckle, L.H.: Neogene Diatom biostratigraphy of ODP Leg 113, Weddell Sea Antarctic Ocean. In: Barker, P.F., Kennett J.P., et al., *Proceeding of the Ocean Drilling Program, Scientific Results, Leg 113*, 113, 761–789, 1990.
- 670 Griener, K. W. and Warny, S.: Nothofagus pollen grain size as a proxy for long-term climate change: An applied study on Eocene, Oligocene, and Miocene sediments from Antarctica, *Rev. Palaeobot. Palynol.*, 221, 138–143, <https://doi.org/10.1016/j.revpalbo.2015.06.003>, 2015.
- Grimalt, J. and Albaigés, J.: Sources and occurrence of C₁₂–C₂₂n-alkane distributions with even carbon-number preference in sedimentary environments, *Geochim. Cosmochim. Acta*, 51(6), 1379–1384, [https://doi.org/10.1016/0016-7037\(87\)90322-X](https://doi.org/10.1016/0016-7037(87)90322-X), 1987.
- 675 Grimm, E. C.: CONISS: a FORTRAN 77 program for stratigraphically constrained cluster analysis by the method of incremental sum of squares, *Comput. Geosci.*, 13(1), 13–35, [https://doi.org/10.1016/0098-3004\(87\)90022-7](https://doi.org/10.1016/0098-3004(87)90022-7), 1987.



- 680 Han, J. and Calvin, M.: HYDROCARBON DISTRIBUTION OF ALGAE AND BACTERIA, AND MICROBIOLOGICAL
ACTIVITY IN SEDIMENTS, *Proc. Natl. Acad. Sci.*, 64(2), 436 LP – 443, <https://doi.org/10.1073/pnas.64.2.436>,
1969.
- Harbert, R. S. and Nixon, K. C.: Climate reconstruction analysis using coexistence likelihood estimation (CRACLE): A method
for the estimation of climate using vegetation, *Am. J. Bot.*, 102(8), 1277–1289, <https://doi.org/10.3732/ajb.1400500>,
2015.
- Hijmans, R. J., Phillips, S., Leathwick, J., and Elith, J.: Species distribution modeling with R, R Packag. version 0.8-11, cran
685 [code], <http://cran.r-project.org/web/packages/dismo/index.html>, 2013.
- Hollis, C. J., Dunkley Jones, T., Anagnostou, E., Bijl, P. K., Cramwinckel, M. J., Cui, Y., Dickens, G. R., Edgar, K. M., Eley,
Y., and Evans, D.: The DeepMIP contribution to PMIP4: methodologies for selection, compilation and analysis of
latest Paleocene and early Eocene climate proxy data, incorporating version 0.1 of the DeepMIP database, *Geosci.
Model Dev.*, 12(7), 3149–3206, <https://doi.org/10.5194/gmd-12-3149-2019>, 2019.
- 690 Houben, A. J. P.: Triggers and consequences of glacial expansion across the Eocene-Oligocene Transition, Ph.D. thesis,
Department of Earth Sciences, Utrecht University, Utrecht, Netherlands, 2012.
- Houben, A. J. P., Bijl, P. K., Pross, J., Bohaty, S. M., Passchier, S., Stickley, C. E., Röhl, U., Sugisaki, S., Tauxe, L., van de
Flierdt, T., Olney, M., Sangiorgi, F., Sluijs, A., Escutia, C., and Brinkhuis, H.: Reorganization of Southern Ocean
Plankton Ecosystem at the Onset of Antarctic Glaciation, *Science*, 340(6130), 341 LP – 344,
695 <https://doi.org/10.1126/science.1223646>, 2013.
- Houben, A. J. P., Bijl, P. K., Sluijs, A., Schouten, S., and Brinkhuis, H.: Late Eocene Southern Ocean Cooling and Invigoration
of Circulation Preconditioned Antarctica for Full-Scale Glaciation, *Geochemistry, Geophys. Geosystems*, 20(5),
2214–2234, <https://doi.org/10.1029/2019GC008182>, 2019.
- Hutchinson, D. K., Coxall, H. K., Lunt, D. J., Steinthorsdottir, M., de Boer, A. M., Baatsen, M., von der Heydt, A., Huber, M.,
700 Kennedy-Asser, A. T., and Kunzmann, L.: The Eocene–Oligocene transition: a review of marine and terrestrial proxy
data, models and model–data comparisons, *Clim. Past*, 17, 269–315, <https://doi.org/10.5194/cp-17-269-2021>, 2021.
- Ivany, L. C., Van Simaey, S., Domack, E. W., and Samson, S. D.: Evidence for an earliest Oligocene ice sheet on the Antarctic
Peninsula, *Geology*, 34(5), 377–380, <https://doi.org/10.1130/G22383.1>, 2006.
- Ivany, L. C., Lohmann, K. C., Hasiuk, F., Blake, D. B., Glass, A., Aronson, R. B., and Moody, R. M.: Eocene climate record
705 of a high southern latitude continental shelf: Seymour Island, Antarctica, *GSA Bull.*, 120(5-6), 659–678,
<https://doi.org/10.1130/B26269.1>, 2008.
- Jahn, B., Donner, B., Müller, P. J., Röhl, U., Schneider, R. R., and Wefer, G.: Pleistocene variations in dust input and marine
productivity in the northern Benguela Current: Evidence of evolution of global glacial–interglacial cycles,
Palaeogeogr. Palaeoclimatol. Palaeoecol., 193(3), 515–533, [https://doi.org/10.1016/S0031-0182\(03\)00264-5](https://doi.org/10.1016/S0031-0182(03)00264-5), 2003.



- 710 Jalali, B., Sicre, M.-A., Kallel, N., Azuara, J., Combourieu-Nebout, N., Bassetti, M.-A., and Klein, V.: High-resolution
Holocene climate and hydrological variability from two major Mediterranean deltas (Nile and Rhone), *The Holocene*,
27(8), 1158–1168, <https://doi.org/10.1177/0959683616683258>, 2017.
- Jalali, B., Sicre, M.-A., Klein, V., Schmidt, S., Maselli, V., Lirer, F., Bassetti, M.-A., Toucanne, S., Jorry, S. J., Insinga, D. D.,
Petrosino, P., and Châles, F.: Deltaic and Coastal Sediments as Recorders of Mediterranean Regional Climate and
715 Human Impact Over the Past Three Millennia, *Paleoceanogr. Paleoclimatology*, 33(6), 579–593,
<https://doi.org/10.1029/2017PA003298>, 2018.
- Juggins, S.: Rioja: analysis of Quaternary science data, R package version (0.9-15.1), <https://cran.r-project.org/web/packages/rioja/index.html>, 2020.
- Kennett, J. P.: Cenozoic evolution of Antarctic glaciation, the circum-Antarctic Ocean, and their impact on global
720 paleoceanography, *J. Geophys. Res.*, 82(27), 3843–3860, <https://doi.org/10.1029/JC082i027p03843>, 1977.
- Kershaw, A.P.: Australasia, in: *Vegetation History*, edited by: Huntley, B., and Webb, T., Kluwer Academic Publisher,
Dordrecht, The Netherlands, pp. 237-306, 1988.
- Kershaw, P. and Wagstaff, B.: The Southern Conifer Family Araucariaceae: History, Status, and Value for Paleoenvironmental
725 Reconstruction, *Annu. Rev. Ecol. Syst.*, 32(1), 397–414, <https://doi.org/10.1146/annurev.ecolsys.32.081501.114059>,
2001.
- King, E. C. and Barker, P. F.: The margins of the South Orkney microcontinent, *J. Geol. Soc. London.*, 145(2), 317 LP – 331,
<https://doi.org/10.1144/gsjgs.145.2.0317>, 1988.
- Kirshner, A. E., Anderson, J. B., and Wellner, J. S.: Cenozoic glacial history of the northern Antarctic Peninsula: a
micromorphological investigation of quartz sand grains, in: *Tectonic, Climatic, and Cryospheric Evolution of the*
730 *Antarctic peninsula*, vol. 63, American Geophysical Union Washington, DC, 153–165, <https://doi.org/10.1029/2010SP001046>, 2011.
- Klages, J. P., Salzmann, U., Bickert, T., Hillenbrand, C.-D., Gohl, K., Kuhn, G., Bohaty, S. M., Titschack, J., Müller, J., and
Frederichs, T.: Temperate rainforests near the South Pole during peak Cretaceous warmth, *Nature*, 580(7801), 81–
86, <https://doi.org/10.1038/s41586-020-2148-5>, 2020.
- 735 Kolattukudy, P.E., Croteau, R., Buckner, J.S., *Biochemistry of plant waxes*, in: *Chemistry and Biochemistry of Natural Waxes*,
edited by: Durig, J. R., and Kolattukudy, P.E., Elsevier Scientific Publishing Company, California, 1976.
- Kühl, N., Gebhardt, C., Litt, T., and Hense, A.: Probability Density Functions as Botanical-Climatological Transfer Functions
for Climate Reconstruction, *Quat. Res.*, 58(3), 381–392, <https://doi.org/10.1006/qres.2002.2380>, 2002.
- Larcher, W. and Winter, A.: Frost susceptibility of palms: experimental data and their interpretation., *Principes*, 25, 143–155,
740 1981.
- Lawver, L. A. and Gahagan, L. M.: Opening of Drake Passage and its impact on Cenozoic ocean circulation, in *Tectonic
Boundary Conditions for Climate Reconstructions*, edited by T. J. Crowley, and K. C. Burke, Oxford Univ. Press,
New York, 212–223, 1998.



- Leathwick, J. R.: Are New Zealand's *Nothofagus* species in equilibrium with their environment?, *J. Veg. Sci.*, 9(5), 719–732,
745 <https://doi.org/10.2307/3237290>, 1998.
- Lewis, A. R., Marchant, D. R., Ashworth, A. C., Hedenäs, L., Hemming, S. R., Johnson, J. V., Leng, M. J., Machlus, M. L.,
Newton, A. E., Raine, J. I., Willenbring, J. K., Williams, M., and Wolfe, A. P.: Mid-Miocene cooling and the
extinction of tundra in continental Antarctica, *Proc. Natl. Acad. Sci.*, 105, 10676–10680,
<https://doi.org/10.1073/pnas.0802501105>, 2008.
- 750 Lepp, A. P.: Geochemical and Sedimentological Analysis of Marine Sediments from ODP Site 696 and Implications for the
Onset of Antarctic Glaciation, M. S. thesis, Montclair State University, Montclair, New Jersey, 2018.
- Liu, Z., Pagani, M., Zinniker, D., DeConto, R., Huber, M., Brinkhuis, H., Shah, S. R., Leckie, R. M., and Pearson, A.: Global
Cooling During the Eocene-Oligocene Climate Transition, *Science*, 323, 1187 LP – 1190,
<https://doi.org/10.1126/science.1166368>, 2009.
- 755 Livermore, R., Hillenbrand, C., Meredith, M., and Eagles, G.: Drake Passage and Cenozoic climate: an open and shut case?,
Geochemistry, Geophys. Geosystems, 8(1), <https://doi.org/10.1029/2005GC001224>, 2007.
- López-Quirós, A., Escutia, C., Sánchez-Navas, A., Nieto, F., Garcia-Casco, A., Martín-Algarra, A., Evangelinos, D., and
Salabarnada, A.: Glaucony authigenesis, maturity and alteration in the Weddell Sea: An indicator of
paleoenvironmental conditions before the onset of Antarctic glaciation, *Sci. Rep.*, 9(1), 13580,
760 <https://doi.org/10.1038/s41598-019-50107-1>, 2019.
- López-Quirós, A., Sánchez-Navas, A., Nieto, F., Escutia, C., 2020. New insights into the nature of glauconite. *American
Mineralogist* 105, 674–686.
- López-Quirós, A., Escutia, C., Etourneau, J., Rodríguez-Tovar, F. J., Roignant, S., Lobo, F. J., Thompson, N., Bijl, P. K.,
Bohoyo, F., Salzmann, U., Evangelinos, D., Salabarnada, A., Hoem, F. S., Sicre, M. A.: Eocene-Oligocene
765 paleoenvironmental changes in the South Orkney Microcontinent (Antarctica) linked to the opening of Powell Basin,
[in review].
- Luo, Q., Zhong, N., Zhu, L., Wang, Y., Qin, J., Qi, L., Zhang, Y., and Ma, Y.: Correlation of burial organic carbon and
paleoproductivity in the Mesoproterozoic Hongshuizhuang Formation, northern North China, *Chinese Sci. Bull.*,
58(11), 1299–1309, 2013.
- 770 Lusk, C. H., Jorgensen, M. A., and Bellingham, P. J.: A conifer–angiosperm divergence in the growth vs. shade tolerance
trade-off underlies the dynamics of a New Zealand warm-temperate rain forest, *J. Ecol.*, 103(2), 479–488,
<https://doi.org/10.1111/1365-2745.12368>, 2015.
- Lyle, M., Murray, D. W., Finney, B. P., Dymond, J., Robbins, J. M., and Brooksforce, K.: The record of Late Pleistocene
biogenic sedimentation in the eastern tropical Pacific Ocean, *Paleoceanography*, 3(1), 39–59,
775 <https://doi.org/10.1029/PA003i001p00039>, 1988.
- Macphail, M. K.: Palynostratigraphy of the murray basin, inland Southeastern Australia, 23(1), 197–240,
<https://doi.org/10.1080/01916122.1999.9989528>, 1999.



- Macphail, M. and Cantrill, D. J.: Age and implications of the Forest Bed, Falkland Islands, southwest Atlantic Ocean: Evidence from fossil pollen and spores, *Palaeogeogr. Palaeoclimatol. Palaeoecol.*, 240(3), 602–629, <https://doi.org/10.1016/j.palaeo.2006.03.010>, 2006.
- Mahiques, M. M. de, Hanebuth, T. J. J., Nagai, R. H., Bicego, M. C., Figueira, R. C. L., Sousa, S. H. M., Burone, L., Franco-Fraguas, P., Taniguchi, S., and Salaroli, A. B.: Inorganic and organic geochemical fingerprinting of sediment sources and ocean circulation on a complex continental margin (São Paulo Bight, Brazil), *Ocean Sci.*, 13, 209–222, <https://doi.org/10.5194/os-13-209-2017>, 2017.
- Meyers, P. A. and Ishiwatari, R.: Lacustrine organic geochemistry—an overview of indicators of organic matter sources and diagenesis in lake sediments, *Org. Geochem.*, 20(7), 867–900, [https://doi.org/10.1016/0146-6380\(93\)90100-P](https://doi.org/10.1016/0146-6380(93)90100-P), 1993.
- Meyers, P. A.: Organic geochemical proxies of paleoceanographic, paleolimnologic, and paleoclimatic processes, *Org. Geochem.*, 27(5), 213–250, [https://doi.org/10.1016/S0146-6380\(97\)00049-1](https://doi.org/10.1016/S0146-6380(97)00049-1), 1997.
- Mohr, B. A. R.: Eocene and Oligocene sporomorphs and dinoflagellate cysts from Leg 113 drill sites, Weddell Sea, Antarctica, in: *Proceedings of the Ocean Drilling Program, scientific results*, 595–612, 1990.
- Moossen, H., Bendle, J., Seki, O., Quillmann, U., and Kawamura, K.: North Atlantic Holocene climate evolution recorded by high-resolution terrestrial and marine biomarker records, *Quat. Sci. Rev.*, 129, 111–127, <https://doi.org/10.1016/j.quascirev.2015.10.013>, 2015.
- Morris, E. K., Caruso, T., Buscot, F., Fischer, M., Hancock, C., Maier, T. S., Meiners, T., Müller, C., Obermaier, E., Prati, D., Socher, S. A., Sonnemann, I., Wäschke, N., Wubet, T., Wurst, S., and Rillig, M. C.: Choosing and using diversity indices: insights for ecological applications from the German Biodiversity Exploratories, *Ecol. Evol.*, 4(18), 3514–3524, <https://doi.org/10.1002/ece3.1155>, 2014.
- Newnham, R., McGlone, M., Moar, N., Wilmshurst, J., and Vandergoes, M.: The vegetation cover of New Zealand at the Last Glacial Maximum, *Quat. Sci. Rev.*, 74, 202–214, <https://doi.org/10.1016/j.quascirev.2012.08.022>, 2013.
- Nichols, J. E., Booth, R. K., Jackson, S. T., Pendall, E. G., and Huang, Y.: Paleohydrologic reconstruction based on n-alkane distributions in ombrotrophic peat, *Org. Geochem.*, 37(11), 1505–1513, <https://doi.org/10.1016/j.orggeochem.2006.06.020>, 2006.
- Nott, C. J., Xie, S., Avsejs, L. A., Maddy, D., Chambers, F. M., and Evershed, R. P.: n-Alkane distributions in ombrotrophic mires as indicators of vegetation change related to climatic variation, *Org. Geochem.*, 31(2), 231–235, [https://doi.org/10.1016/S0146-6380\(99\)00153-9](https://doi.org/10.1016/S0146-6380(99)00153-9), 2000.
- Oksanen, J., Blanchet, F. G., Kindt, R., Legendre, P., Minchin, P. R., O’hara, R. B., Simpson, G. L., Solymos, P., Stevens, M. H. H., and Wagner, H.: Package ‘vegan,’ Community ecology package, version 2.5-7, cran [code], 2013.
- Pancost, R. D., Baas, M., van Geel, B., and Sinninghe Damsté, J. S.: Biomarkers as proxies for plant inputs to peats: an example from a sub-boreal ombrotrophic bog, *Org. Geochem.*, 33(7), 675–690, [https://doi.org/10.1016/S0146-6380\(02\)00048-7](https://doi.org/10.1016/S0146-6380(02)00048-7), 2002.



- Poole, A.L.: Southern beeches, Science Information Publishing Centre, DSIR information series no. 162, Wellington, New Zealand, 1987.
- Poole, I., Hunt, R. J., and Cantrill, D. J.: A Fossil Wood Flora from King George Island: Ecological Implications for an Antarctic Eocene Vegetation, *Ann. Bot.*, 88(1), 33–54, <https://doi.org/10.1006/anbo.2001.1425>, 2001.
- 815 Poole, I., Mennega, A. M. W., and Cantrill, D. J.: Valdivian ecosystems in the Late Cretaceous and Early Tertiary of Antarctica: further evidence from myrtaceous and eucryphiaceous fossil wood, *Rev. Palaeobot. Palynol.*, 124(1), 9–27, [https://doi.org/10.1016/S0034-6667\(02\)00244-0](https://doi.org/10.1016/S0034-6667(02)00244-0), 2003.
- Poynter, J. G., Farrimond, P., Robinson, N., and Eglinton, G.: Aeolian-Derived Higher Plant Lipids in the Marine Sedimentary Record: Links with Palaeoclimate, in: *Paleoclimatology and Paleometeorology: Modern and Past Patterns of Global Atmospheric Transport*, edited by: Leinen, M. and Sarinthein, M., Springer Netherlands, Dordrecht, 435–462, 820 https://doi.org/10.1007/978-94-009-0995-3_18, 1989.
- Prebble, J. G., Raine, J. I., Barrett, P. J., and Hannah, M. J.: Vegetation and climate from two Oligocene glacioeustatic sedimentary cycles (31 and 24 Ma) cored by the Cape Roberts Project, Victoria Land Basin, Antarctica, *Palaeogeogr. Palaeoclimatol. Palaeoecol.*, 231(1), 41–57, <https://doi.org/10.1016/j.palaeo.2005.07.025>, 2006.
- 825 Pross, J., Contreras, L., Bijl, P. K., Greenwood, D. R., Bohaty, S. M., Schouten, S., Bendle, J. A., Röhl, U., Tauxe, L., Raine, J. I., Huck, C. E., van de Flierdt, T., Jamieson, S. S. R., Stickley, C. E., van de Schootbrugge, B., Escutia, C., Brinkhuis, H., Brinkhuis, H., Escutia Dotti, C., Klaus, A., Fehr, A., Williams, T., Bendle, J. A. P., Bijl, P. K., Bohaty, S. M., Carr, S. A., Dunbar, R. B., González, J. J., Hayden, T. G., Iwai, M., Jimenez-Espejo, F. J., Katsuki, K., Soo Kong, G., McKay, R. M., Nakai, M., Olney, M. P., Passchier, S., Pekar, S. F., Pross, J., Riesselman, C. R., Röhl, U., 830 Sakai, T., Shrivastava, P. K., Stickley, C. E., Sugisaki, S., Tauxe, L., Tuo, S., van de Flierdt, T., Welsh, K., Yamane, M., and Scientists, I. O. D. P. E. 318: Persistent near-tropical warmth on the Antarctic continent during the early Eocene epoch, *Nature*, 488(7409), 73–77, <https://doi.org/10.1038/nature11300>, 2012.
- Punyasena, S.W., Dalling, J.W., Jaramillo, C., Turner, B.L.: The response of vegetation on the Andean flank in western Amazonia to Pleistocene climate change, *Science*, 331(6020), 1055–1058, <https://doi.org/10.1126/science.1197947>, 835 2011.
- R Development Core Team: R: A language and environment for statistical computing, 2013.
- Raine, J. I.: Terrestrial palynomorphs from Cape Roberts Project drillhole CRP-1, Ross Sea, Antarctica, *Terra Antart.*, 5(3), 539–548, 1998.
- Raine, J. I. and Askin, R. A.: Terrestrial palynology of Cape Roberts Project drillhole CRP-3, Victoria Land Basin, Antarctica, 840 *Terra Antart.*, 8, 389–400, 2001.
- Raine, J.I., Mildenhall, D.C. and Kennedy, E.: New Zealand fossil spores and pollen: an illustrated catalogue, https://www.gns.cri.nz/what/earthhist/fossils/spore_pollen/catalog/index.htm, 2011.
- Raup, D. M.: Taxonomic diversity estimation using rarefaction, *Paleobiology*, 333–342, 1975.



- Rawlence, N. J., Potter, B. C. M., Dussex, N., Scarsbrook, L., Orlovich, D. A., Waters, J. M., McGlone, M., and Knapp, M.:
845 Plio-Pleistocene environmental changes shape present day phylogeography of New Zealand's southern beeches
(Nothofagaceae), *New Zeal. J. Bot.*, 59(1), 55–71, <https://doi.org/10.1080/0028825X.2020.1791915>, 2021.
- Reichgelt, T., Kennedy, E. M., Jones, W. A., Jones, D. T., and Lee, D. E.: Contrasting palaeoenvironments of the mid/late
Miocene Dunedin Volcano, southern New Zealand: Climate or topography?, *Palaeogeogr. Palaeoclimatol.*
Palaeoecol., 441, 696–703, <https://doi.org/10.1016/j.palaeo.2015.10.029>, 2016.
- 850 Reichgelt, T., West, C. K., and Greenwood, D. R.: The relation between global palm distribution and climate, *Sci. Rep.*, 8(1),
4721, <https://doi.org/10.1038/s41598-018-23147-2>, 2018.
- Rielley, G., Collier, R. J., Jones, D. M., and Eglinton, G.: The biogeochemistry of Ellesmere Lake, U.K.—I: source correlation
of leaf wax inputs to the sedimentary lipid record, *Org. Geochem.*, 17(6), 901–912, [https://doi.org/10.1016/0146-6380\(91\)90031-E](https://doi.org/10.1016/0146-6380(91)90031-E), 1991.
- 855 Robert, C. and Mailliot, H.: Palaeoenvironments in the Weddell Sea area and Antarctic climates, as deduced from clay mineral
associations and geochemical data, ODP Leg 113, in: *Proceedings of the Ocean Drilling Program, scientific results*,
51–66, 1990.
- Romero, E. J. and Zamalao, M. C.: Polen de Angiospermas de la Formacion Rio Turbio (Eoceno), Provincia de Santa Cruz,
Republica Argentina, *Ameghiniana*, 22 (1-2), 43-51, 1985.
- 860 Romero, E.J. and Castro, M.T.: Material fúngico y granos de polen de angiospermas de la Formación Río Turbio (Eoceno),
provincial de Santa Cruz, República Argentina, *Ameghiniana*, 23(1-2), 101-118, 1986.
- Rommerskirchen, F., Eglinton, G., Dupont, L., and Rullkötter, J.: Glacial/interglacial changes in southern Africa: Compound-
specific $\delta^{13}\text{C}$ land plant biomarker and pollen records from southeast Atlantic continental margin sediments,
Geochemistry, Geophys. Geosystems, 7(8), <https://doi.org/10.1029/2005GC001223>, 2006.
- 865 Sangiorgi, F., Bijl, P. K., Passchier, S., Salzmann, U., Schouten, S., McKay, R., Cody, R. D., Pross, J., van de Flierdt, T.,
Bohaty, S. M., Levy, R., Williams, T., Escutia, C., and Brinkhuis, H.: Southern Ocean warming and Wilkes Land ice
sheet retreat during the mid-Miocene, *Nat. Commun.*, 9(1), 317, <https://doi.org/10.1038/s41467-017-02609-7>, 2018.
- Sarkar, S., Basak, C., Frank, M., Berndt, C., Huuse, M., Badhani, S., and Bialas, J.: Late Eocene onset of the Proto-Antarctic
Circumpolar Current, *Sci. Rep.*, 9(1), 10125, <https://doi.org/10.1038/s41598-019-46253-1>, 2019.
- 870 Sarnthein, M., Winn, K., Duplessy, J.-C., and Fontugne, M. R.: Global variations of surface ocean productivity in low and mid
latitudes: Influence on CO₂ reservoirs of the deep ocean and atmosphere during the last 21,000 years,
Paleoceanography, 3(3), 361–399, <https://doi.org/10.1029/PA003i003p00361>, 1988.
- Schefuß, E., Ratmeyer, V., Stuut, J.-B. W., Jansen, J. H. F., and Sinninghe Damsté, J. S.: Carbon isotope analyses of n-alkanes
in dust from the lower atmosphere over the central eastern Atlantic, *Geochim. Cosmochim. Acta*, 67(10), 1757–1767,
875 [https://doi.org/10.1016/S0016-7037\(02\)01414-X](https://doi.org/10.1016/S0016-7037(02)01414-X), 2003.



- Scher, H. D. and Martin, E. E.: Oligocene deep water export from the North Atlantic and the development of the Antarctic Circumpolar Current examined with neodymium isotopes, *Paleoceanography*, 23, <https://doi.org/10.1029/2006PA001400>, 2008.
- Shannon, C. E.: A mathematical theory of communication, *Bell Syst. Tech. J.*, 27(3), 379–423, <https://doi.org/10.1002/j.1538-7305.1948.tb01338.x>, 1948.
- 880
- Sicre, M.-A. and Peltzer, E. T.: Lipid geochemistry of remote aerosols from the southwestern Pacific Ocean sector, *Atmos. Environ.*, 38(11), 1615–1624, <https://doi.org/10.1016/j.atmosenv.2003.12.012>, 2004.
- Specht, R. L., Dettmann, M. E., and Jarzen, D. M.: Community associations and structure in the Late Cretaceous vegetation of southeast Australasia and Antarctica, *Palaeogeogr. Palaeoclimatol. Palaeoecol.*, 94(1), 283–309, [https://doi.org/10.1016/0031-0182\(92\)90124-N](https://doi.org/10.1016/0031-0182(92)90124-N), 1992.
- 885
- Thompson, N., Salzmann, U., López-Quirós, A., Bijl, P. K., Hoem, F. S., Etourneau, J., Marie-Alexandrine, S., Roignant, S., Hocking, E., Amoo, M., Escutia, C.: ODP Site 696B Sporomorph Count data, Diversity, DCA and Climate estimate calculations, PANGAEA [data set], awaiting validation.
- Tomlinson, P. B.: The uniqueness of palms, *Bot. J. Linn. Soc.*, 151(1), 5–14, <https://doi.org/10.1111/j.1095-8339.2006.00520.x>, 2006.
- 890
- Traverse, A. (Eds): *Paleopalynology* (Vol. 28), Springer Science & Business Media, 2007.
- Truswell, E. M. and Macphail, M. K.: Polar forests on the edge of extinction: what does the fossil spore and pollen evidence from East Antarctica say?, *Aust. Syst. Bot.*, 22(2), 57–106, <https://doi.org/10.1071/SB08046>, 2009.
- van de Lagemaat, S. H. A., Swart, M. L. A., Vaes, B., Kusters, M. E., Boschman, L. M., Burton-Johnson, A., Bijl, P. K., Spakman, W., and van Hinsbergen, D. J. J.: Subduction initiation in the Scotia Sea region and opening of the Drake Passage: When and why?, *Earth-Sci. Rev.*, 215, 103551, <https://doi.org/10.1016/j.earscirev.2021.103551>, 2021.
- 895
- Veblen, T.T., Schlegel, F. M., Oltremari, V. J.: Temperate broad-leaved evergreen forests of South America, in: *Temperate Broad-Leaved Forests*, edited by: Ovington, J. D., Elsevier, Amsterdam, Netherlands, 5-31, 1983.
- Veblen, T. T., Donoso, C., Kitzberger, T., and Rebertus, A. J.: Ecology of southern Chilean and Argentinean *Nothofagus* forests, *Ecol. Biogeogr. Nothofagus For.*, 10, 93–353, 1996.
- 900
- Villa, G., Fioroni, C., Pea, L., Bohaty, S., and Persico, D.: Middle Eocene–late Oligocene climate variability: calcareous nannofossil response at Kerguelen Plateau, Site 748, *Mar. Micropaleontol.*, 69, 173–192, <https://doi.org/10.1016/j.marmicro.2008.07.006>, 2008.
- Vogts, A., Moossen, H., Rommerskirchen, F., and Rullkötter, J.: Distribution patterns and stable carbon isotopic composition of alkanes and alkan-1-ols from plant waxes of African rain forest and savanna C3 species, *Org. Geochem.*, 40(10), 1037–1054, <https://doi.org/10.1016/j.orggeochem.2009.07.011>, 2009.
- 905
- Wardle, J.: *The New Zealand beeches: ecology, utilisation and management.*, New Zealand Forest Service, 1984.
- Warny, S., Askin, R., Anderson, J. B., and Wellner, J. S.: Vegetation and organic-walled phytoplankton at the end of the Antarctic greenhouse world: Latest Eocene cooling events, in: *Tectonic, Climatic, and Cryospheric Evolution of the*



- 910 Antarctic peninsula, vol. 63, American Geophysical Union Washington, DC, 63, 193–210,
<https://doi.org/10.1029/2010SP000965>, 2011a.
- Warny, S. and Askin, R.: Last remnants of Cenozoic vegetation and organic-walled phytoplankton in the Antarctic Peninsula's icehouse world, in: Tectonic, Climatic, and Cryospheric Evolution of the Antarctic peninsula, vol. 63, American Geophysical Union Washington, DC, 167–192, <https://doi.org/10.1029/2010SP000996>, 2011b.
- 915 Warny, S., Kymes, C. M., Askin, R., Krajewski, K. P., and Tatur, A.: Terrestrial and marine floral response to latest Eocene and Oligocene events on the Antarctic Peninsula, 43(1), 4–21, <https://doi.org/10.1080/01916122.2017.1418444>, 2019.
- Wei, W. and Wise, S.: Middle Eocene to Pleistocene calcareous nannofossils recovered by ocean drilling program leg 113 in the Weddell Sea, in: Proceedings of the Ocean Drilling Program, scientific results, 639–666, 1990.
- 920 Wellner, J. S., Anderson, J. B., Ehrmann, W., Weaver, F. M., Kirshner, A., Livsey, D., and Simms, A. R.: History of an evolving ice sheet as recorded in SHALDRIL cores from the northwestern Weddell Sea, Antarctica, in: Tectonic, Climatic, and Cryospheric Evolution of the Antarctic peninsula, vol. 63, American Geophysical Union Washington, DC, 131–152, <https://doi.org/10.1029/2010SP001047>, 2011.
- Westerhold, T., Marwan, N., Drury, A. J., Liebrand, D., Agnini, C., Anagnostou, E., Barnet, J. S. K., Bohaty, S. M., De
925 Vleeschouwer, D., Florindo, F., Frederichs, T., Hodell, D. A., Holbourn, A. E., Kroon, D., Laurentano, V., Littler, K., Lourens, L. J., Lyle, M., Pälike, H., Röhl, U., Tian, J., Wilkens, R. H., Wilson, P. A., and Zachos, J. C.: An astronomically dated record of Earth's climate and its predictability over the last 66 million years, *Science*, 369(6509), 1383 LP – 1387, <https://doi.org/10.1126/science.aba6853>, 2020.
- Wigley, R. A. and Compton, J. S.: Late Cenozoic evolution of the outer continental shelf at the head of the Cape Canyon,
930 South Africa, *Mar. Geol.*, 226(1-2), 1–23, <https://doi.org/10.1016/j.margeo.2005.09.015>, 2006.
- Willard, D. A., Donders, T. H., Reichgelt, T., Greenwood, D. R., Sangiorgi, F., Peterse, F., Nierop, K. G. J., Frieling, J., Schouten, S., and Sluijs, A.: Arctic vegetation, temperature, and hydrology during Early Eocene transient global warming events, *Glob. Planet. Change*, 178, 139–152, <https://doi.org/10.1016/j.gloplacha.2019.04.012>, 2019.
- Wilson, D. S., Jamieson, S. S. R., Barrett, P. J., Leitchenkov, G., Gohl, K., and Larter, R. D.: Antarctic topography at the
935 Eocene–Oligocene boundary, *Palaeogeogr. Palaeoclimatol. Palaeoecol.*, 335–336, 24–34, <https://doi.org/10.1016/j.palaeo.2011.05.028>, 2012.
- Wilson, D. S., Pollard, D., DeConto, R. M., Jamieson, S. S. R., and Luyendyk, B. P.: Initiation of the West Antarctic Ice Sheet and estimates of total Antarctic ice volume in the earliest Oligocene, *Geophys. Res. Lett.*, 40(16), 4305–4309, <https://doi.org/10.1002/grl.50797>, 2013.
- 940 Zachos, J., Pagani, M., Sloan, L., Thomas, E., and Billups, K.: Trends, Rhythms, and Aberrations in Global Climate 65 Ma to Present, *Science*, 292(5517), 686 LP – 693, <https://doi.org/10.1126/science.1059412>, 2001.
- Zachos, J. C., Dickens, G. R., and Zeebe, R. E.: An early Cenozoic perspective on greenhouse warming and carbon-cycle dynamics, *Nature*, 451(7176), 279–283, <https://doi.org/10.1038/nature06588>, 2008.



- Zhang, R. and Delworth, T. L.: Simulated tropical response to a substantial weakening of the Atlantic thermohaline circulation, *J. Clim.*, 18(12), 1853–1860, 2005.
- Zhou, W., Xie, S., Meyers, P. A., and Zheng, Y.: Reconstruction of late glacial and Holocene climate evolution in southern China from geolipids and pollen in the Dingnan peat sequence, *Org. Geochem.*, 36(9), 1272–1284, <https://doi.org/10.1016/j.orggeochem.2005.04.005>, 2005.

Table captions

- 950 **Table 1: Revised age model for Ocean Drilling Program (ODP) Leg 113 Site determined by calcareous nannofossil and dinoflagellate cysts biostratigraphy (FO = First occurrence, FCO = First common occurrence)**
- Table 2: List of fossil pollen and spore taxa and their NLR used in sporomorph-based climate estimates from ODP Site 696.**

Figure captions

- 955 **Figure 1: Modern day geographical and tectonic setting of the study area, showing location of ODP Site 696 on the southeastern margin of the SOM (red circle), and litho-tectonic units superimposed for the Antarctic Peninsula and southern South America (modified after Elliot, 1988). Tectonic setting and features after Maldonado et al. (2015). APR, Antarctic-Phoenix Ridge; BB, Bruce Bank; Sea; DB, Discovery Bank; DvB, Dove Basin; EB, Endurance Basin; ESR, East Scotia Ridge; FP, Falkland Plateau; HB, Herman Bank; JB, Jane Basin; JBk, Jane Bank; OB, Ona Basin; PB, Powell Basin; PBk, Protector Bank; PrB, Protector Basin; SB, Scan Basin; SGM, South Georgia Microcontinent; SI, Seymour Island; SOM, South Orkney Microcontinent; SSIB, South Shetland Islands Block; TR, Terror Rise; WSR, West Scotia Ridge; and WSS, West Scotia Sea. (Adapted from López-Quirós et al., 2019, in review).**

- 960 **Figure 2: Stratigraphy of the studied sedimentary interval from ODP Site 696 Hole B. From left to right: Simplified lithological log of ODP Site 696, Age-depth plot based on biostratigraphy, cores, detailed lithological log of Eocene-Oligocene Unit VII and clay mineral percentage. Biostratigraphic age constraints based on calcareous nannofossils (Wei and Wise, 1990) and dinoflagellate cysts (Houben et al., 2013). Detailed lithological log from López-Quirós et al. (2019, in review). Clay minerals are from Robert and Maillot (1990). (Adapted from López-Quirós et al., 2019, in review).**

- Figure 3: Frequency and stratigraphic distribution of major pollen and spore taxa with CONISS ordination showing two distinct zones (Zone I and Zone II), Zone I further subdivided based on the occurrence of key taxa. Pollen and spore taxa have been separated into key ecological groups.**

- 970 **Figure 4: Sporomorph based quantitative climate estimates using probability density functions (PDF). From left to right: Coldest Month Mean Temperature (CMMT), Mean Annual Temperature (MAT), Warmest Month Mean Temperature (WMMT) and Mean Annual Precipitation (MAP).**

- 975 **Figure 5: Distribution of key vegetation and dinocyst groups plotted against diversity indices results, percentages of reworked terrestrial palynomorphs and *n*-alkane variables/ratios. From left to right: Rarefaction analysis results at number of species per 50 and 100 specimens, percentage of reworked terrestrial palynomorphs, DCA axis 1 results, percentage of cryptogam taxa, percentage of angiosperm taxa (non-*Nothofagus*), percentage of gymnosperm taxa, percentage of *Nothofagus*, percentage of endemic-Antarctic dinocyst taxa, percentage of Protoperidiniaceae dinoflagellates, TOC, TI index, ACL, Paq and *n*-alkane *n*-C23/*n*-C29 ratios. Dinoflagellate abundance from Houben et al. (2013). Terrestrial biomarkers/*n*-alkane variables/ratios from López-Quirós et al. (in review).**

- 980 **Figure 6: Schematic representation of vegetation from Site 696, illustrating the response of key taxonomic group to climate and environmental change through key intervals during the late Eocene and early Oligocene. (A) Late Eocene vegetation (~37.6–35.5 Ma), during the deposition of Zone Ia vegetation was dominated by *Nothofagus* with secondary podocarps and an understory of cryptogams and minor angiosperms. Sporomorph-based climate estimates and the presence of paratropical taxa indicate conditions were relatively warm compared to the rest of the section; (B) Latest Eocene after late Eocene climate cooling (~35.5–34.1 Ma), vegetation remained similar to that of the late Eocene and was still dominated by *Nothofagus*, but climate cooling by around 2°C**
- 985



990 **resulted in loss of paratropical taxa and slight decrease in taxa diversity; (C) EOT vegetation during glacial onset (~34.1 Ma), environmental disturbance caused by ice expansion and retreat resulted in the reduction of *Nothofagus*-dominated forested areas and increase in tundra-like vegetation; (D) early Oligocene (~33.5-32.2 Ma), during glacial retreat and the development of milder climates disturbance and reduction of *Nothofagus*-dominated forests facilitated the expansion of more competitive Podocarpaceae and pioneer cryptogam taxa.**

995

1000

1005

1010

1015



Table 1

Event/Characteristic	Kind	Lower level	Upper level	Bottom depth	Top depth	Mid-depth	Reference	Age (Ma)	Reference
<i>FO Chiropteridium galea</i>	Dinocysts	53R-3, 80 cm	53R-2, 130 cm	552.70	551.70	552.20	Houben et al., 2019	<33.26	Pross et al., 2010
<i>FO Malvinia escutiana</i>	Dinocysts	55R-1, 117 cm	55R-1, 62 cm	569.39	568.82	569.11	Houben et al., 2013; 2019	33.6	Houben et al., 2011
<i>FO Stoveracysta kakanuiensis</i>	Dinocysts	55R-3, 75 cm	55R-2, 147 cm	571.95	571.16	571.55	Houben et al., 2013; 2019	34.1	Clowes, 1985
<i>FO Reticulofenestra oamaruensis</i>	Calcareous nannofossils	58R-1, 122cm	57R-1, 112 cm	598.42	588.72	593.57	Wei and Wise, 1990	35.5	Villa et al., 2008
<i>FCO Isthmolithus recurvus</i>	Calcareous nannofossils	60R-1, 36 cm	59R-CC	616.96	616.6	616.78	Wei and Wise, 1990	36.27	Villa et al., 2008
<i>FO Reticulofenestra bisecta</i>	Calcareous nannofossils	62R-6, 132 cm	-	643.62	-	643.62	Wei and Wise, 1990	<37.61	Villa et al., 2008

1020

1025

1030

1035



Table 2

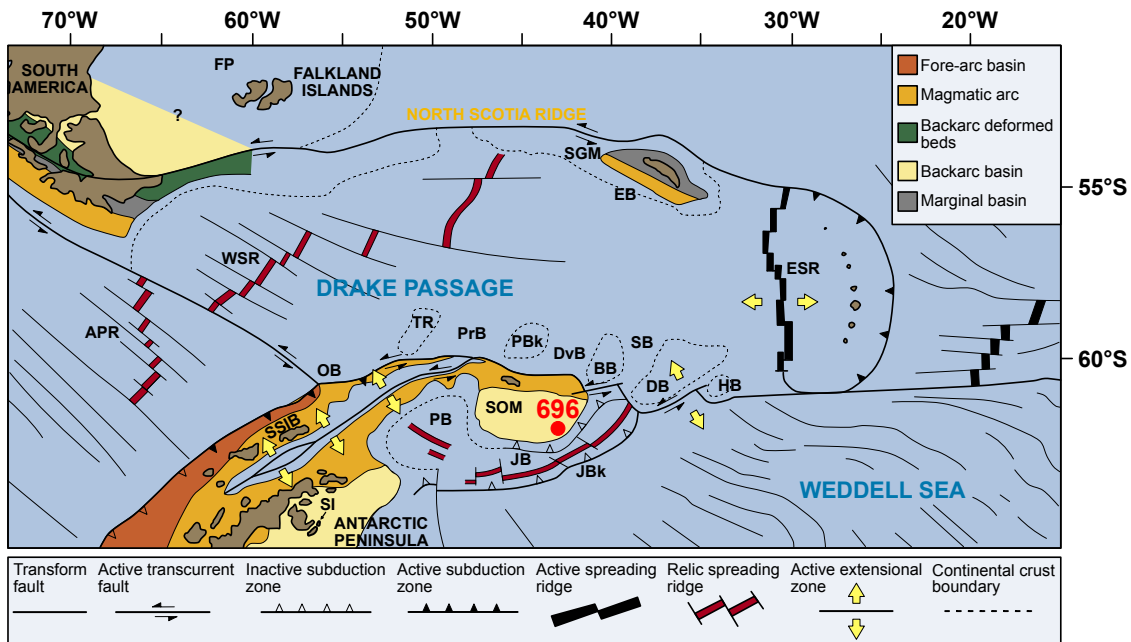
Fossil taxa	Botanical affinity	Reference	NLR used for climate analysis
Angiosperms			
<i>Acaena</i> sp.	<i>Acaena</i>		<i>Acaena</i>
<i>Arecipites</i> sp.	Arecaceae	Raine et al. (2011)	Arecaceae
<i>Beaupreadites</i> cf. <i>verrucosus</i>	Proteaceae (<i>Beauprea</i>).	Raine et al. (2011)	<i>Beauprea</i>
<i>Chenopodipollis</i> <i>chenopodiaceoides</i>	Chenopodiaceae	Raine et al. (2011)	Chenopodiaceae
<i>Clavatipollenites</i> <i>ascarinoides</i>	Chloranthaceae (<i>Ascarina</i>).	Raine et al. (2011)	<i>Ascarina</i>
<i>Cupanieidites</i> <i>orthoteichus</i>	Sapindaceae	Raine et al. (2011)	Sapindaceae
<i>Ericipites</i> cf. <i>scabratus</i>	Ericaceae	Raine et al. (2011)	Ericaceae
<i>Lateropora</i> <i>glabra</i>	Pandanaceae (<i>Freycinetia</i>)	Raine et al. (2011)	<i>Freycinetia</i>
<i>Liliacidites</i> <i>intermedius</i>	Liliaceae (? <i>Arthropodium</i>)	Raine et al. (2011)	Liliaceae
<i>Lymingtonia</i> cf. <i>cenozoica</i>	Nyctaginaceae (<i>Pisonia brunoniana</i>)	Raine et al. (2011)	<i>Pisonia</i>
<i>Malvacipollis</i> cf. <i>subtilis</i>	Malvaceae?/Euphorbiaceae	Raine et al. (2011)	Euphorbiaceae
<i>Myricipites</i> <i>harrisii</i>	Casuarinaceae/Myricaceae	Raine et al. (2011)	Myricaceae
<i>Myrtacidites</i> cf. <i>mesonesus</i>	Myrtaceae (<i>Metrosideros</i>)	Raine et al. (2011)	<i>Metrosideros</i>
<i>Nothofagidites</i> spp.	Nothofagaceae	Truswell & Macphail (2009)	Nothofagaceae
<i>Propylipollis</i> <i>reticulosabratus</i>	Proteaceae (<i>Gevuina/Hicksbeachia</i>)	Raine et al. (2011)	Proteaceae
<i>Proteacidites</i> spp.	Proteaceae	Truswell & Macphail (2009)	Proteaceae
<i>Sparganiaceapollenites</i> <i>barungensis</i>	Sparganiaceae (<i>Sparganium</i>)	Macphail & Cantrill (2006)	<i>Sparganium</i>
Gymnosperms			
<i>Dacrydimites</i> <i>praecupressinoides</i>	Podocarpaceae (<i>Dacrydium cupressinum</i>)	Raine et al. (2011)	<i>Dacrydium</i>
<i>Microalatiidites</i> <i>paleogenicus</i>	Podocarpaceae (<i>Phyllocladus</i>)	Raine et al. (2011)	<i>Phyllocladus</i>
<i>Microcachryidites</i> <i>antarcticus</i>	Podocarpaceae (<i>Microcachrys tetragona</i>)	Raine et al. (2011)	Podocarpaceae
<i>Phyllocladidites</i> <i>mawsonii</i>	Podocarpaceae (<i>Lagarostrobos franklinii</i>).	Truswell & Macphail (2009)	<i>Lagarostrobos franklinii</i>
<i>Podocarpidites</i> spp.	Podocarpaceae (<i>Podocarpus</i>)	Truswell & Macphail (2009)	<i>Podocarpus</i>
<i>Podosporites</i> spp.	Podocarpaceae (cf. <i>Microcachrys</i>)	Raine et al. (2011)	Podocarpaceae
<i>Trichotomosulcites</i> <i>subgranulatus</i>	Podocarpaceae (<i>Microcachrys</i>)	Raine et al. (2011)	Podocarpaceae
Cryptogams			
<i>Baculatisporites</i> <i>comaumensis</i>	Osmundaceae (<i>Osmunda/Leptopteris</i>)	Raine et al. (2011)	Osmundaceae
<i>Ceratosporites</i> cf. <i>equalis</i>	Selaginellaceae (<i>Selaginella</i>)	Raine et al. (2011)	Selaginellaceae
<i>Coptospora</i> <i>archangelskyi</i>	Bartramiaceae (<i>Conostomum</i>)	Raine (1998)	<i>Conostomum</i>
<i>Cyathidites</i> spp.	Cyatheaceae	Raine et al. (2011)	Cyatheaceae
<i>Dictyophyllidites</i> <i>arcuatus</i>	Gleicheniaceae (? <i>Dicranopteris</i>)	Raine et al. (2011)	<i>Dicranopteris</i>
<i>Foveotrilletes</i> <i>lacunosus</i>	Lycopodiaceae (<i>Huperzia</i>)	Raine et al. (2011)	<i>Huperzia</i>
<i>Gleicheniidites</i> spp.	Gleicheniaceae	Truswell & Macphail (2009)	Gleicheniaceae
<i>Laevigatosporites</i> spp.	Blechnaceae	Truswell & Macphail (2009)	Blechnaceae
<i>Monolites</i> <i>alveolatus</i>	cf. Polypodiaceae (<i>Belvisia</i>)	Raine et al. (2011)	<i>Belvisia</i>
<i>Osmundacidites</i> cf. <i>wellmanii</i>	Osmundaceae (<i>Todea barbara</i>)	Raine et al. (2011)	Osmundaceae
<i>Polypodiisporites</i> cf. <i>radiatus</i>	Davalliaceae (<i>Davallia</i>)	Conran et al. (2010)	<i>Davallia</i>
<i>Retitriletes/Lycopodiacidites</i>	Lycopodiaceae (<i>Lycopodium</i>)	Raine et al. (2011)	<i>Lycopodium</i>
<i>Stereisporites</i> spp.	Sphagnaceae (<i>Sphagnum</i>)	Truswell & Macphail (2009)	<i>Sphagnum</i>

1040

1045



Figure 1



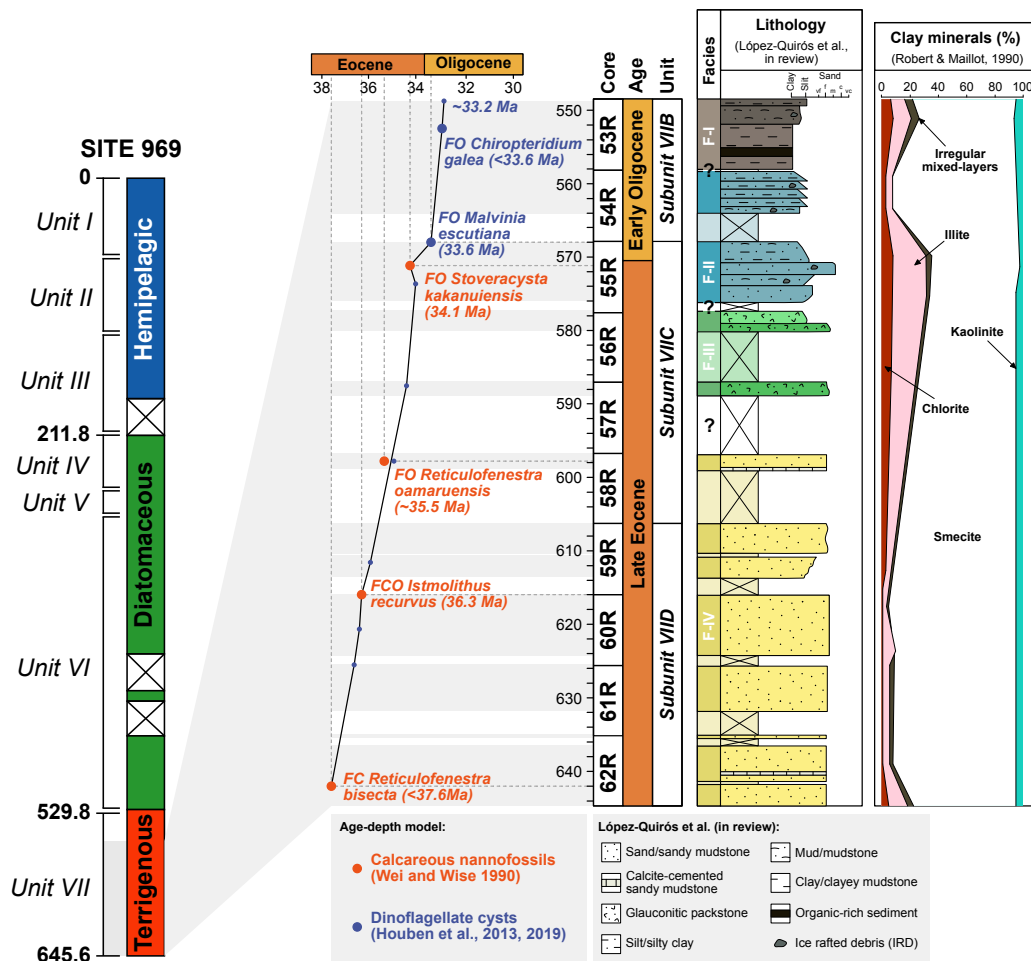
1050

1055

1060



1065 Figure 2

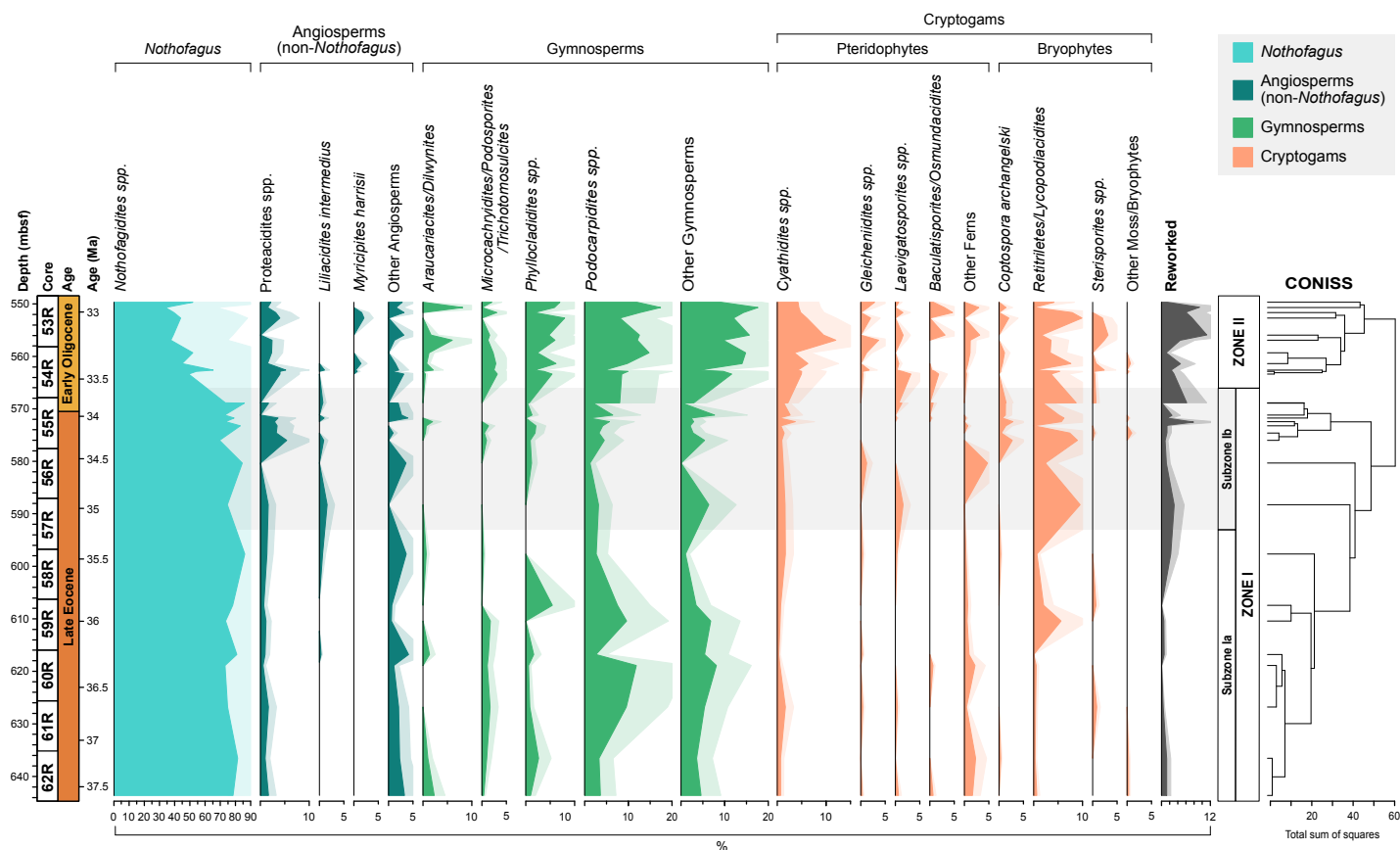


1070

1075



Figure 3

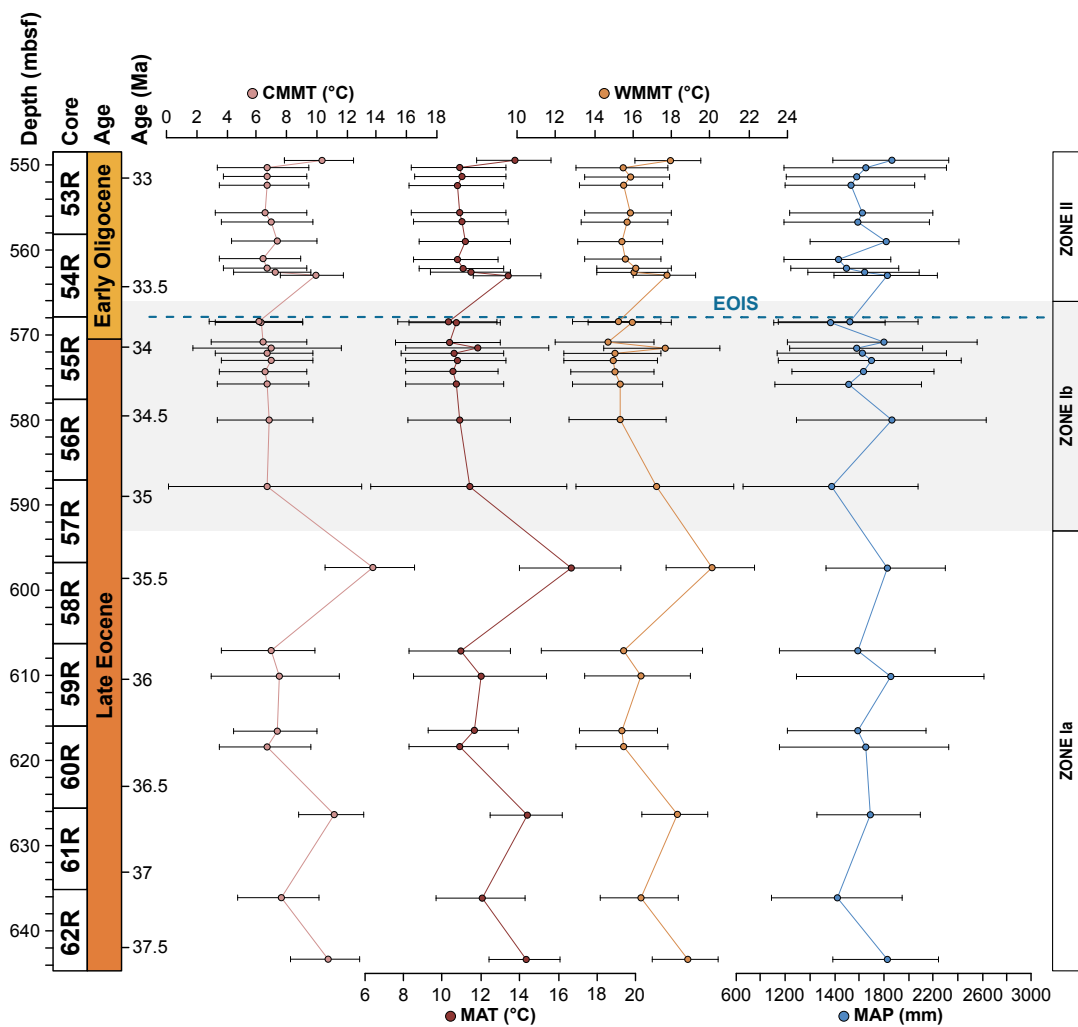


1080

1085



Figure 4

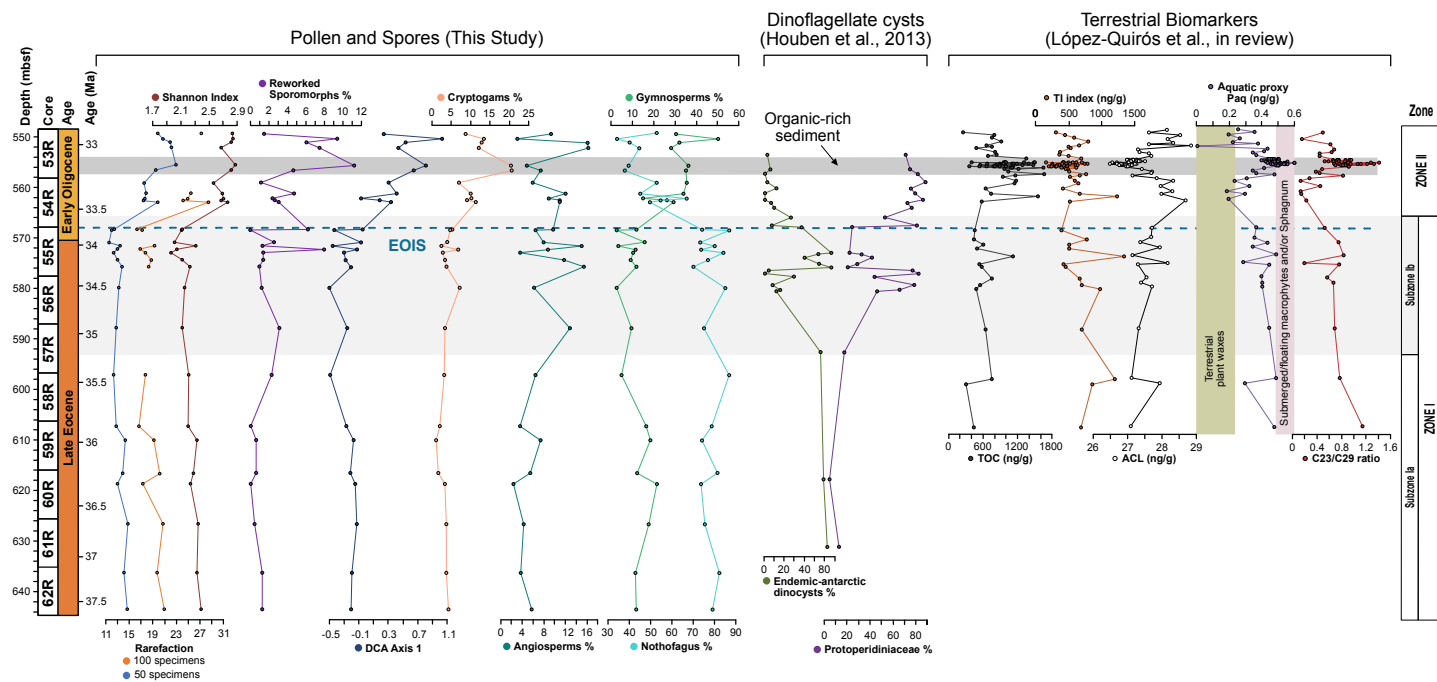


1090

1095



Figure 5



1100

1105

1110

1115



Figure 6

